Petrofabric Study of a Peridotite Nodule from Ichinomegata, Japan*

By

Gensei YOSHINO

with 26 Text-figures and 2 Plates

ABSTRACT: In a lherzolitic peridotite nodule from Ichinomegata, two or more planar structures can be discerned as defined by the preferred location of olivine grains belonging to the different individual direction groups as well as by the grain boundary fabric of olivine. Preferred lattice orientation of olivine in the peridotite nodule does not always correspond with the grain boundary fabric of olivine. The fabrics of orthopyroxene and clinopyroxene in the nodule are inconsistent with the olivine fabric. The olivine fabric may have been developed through the deformation under dry condition. It is likely that the lattice orientation of both pyroxenes is not related to the condition of deformation reflected on the olivine fabric. The earlier structure developed prior to the deformation may have been inherited in the observed state of preferred lattice orientation of both pyroxenes.

CONTENTS

I. INTRODUCTION

Peridotite nodules, accompanied by other rock inclusions, occur in basaltic lapilli and accidental tuff breccia from Ichinomegata, Akita Prefecture. HAYASHI (1955) described those rock fragments or nodules from Ichinomegata, and regarded the olivine nodules as cumulates from primary basaltic magma. KUNO (1967) discussed the chemistry and mineralogy of peridotite and garnet peridotite from Ichinomegata, and said, "it is possible that the analyzed Ichinomegata peridotite is a residual material of partial melting which took place in the past."

Though there are many references to mineralogy and geochemistry of peridotite nodules in volcanic rocks, only a few refer to the petrofabric features (ERNST, 1935, 1967; TURNER, 1942; COLLÉE, 1962; BROTHERS and RODGERS, 1969). The pres-

* Dedicated to the late Prof. Hisashi KUNO.

ent paper deals with the petrofabric of a peridotite nodule collected by H. KUNO from Ichinomegata.

KUNO (1967) has described Ichinomegata as follows: "Ichinome-gata is a circular crater 800 m in diameter lying in Oga Peninsula, Akita Prefecture, northeast Honshu. There are three other craters of similar size in the vicinity. Ichinome-gata is surrounded by deposits of basalt lapilli and accidental tuff breccia ejected from the crater about 4000 years ago (HAYASHI, 1955). They are underlain by older Miocene andesite complex. The deposits contain fragments of the andesite and of less abundant granodiorite, gabbro, hornblende gabbro, pyroxenite, peridotite, and garnet peridotite. The granodiorite was probably derived from the one exposed to the northwest of the crater. The other rock fragments or nodules probably came from deep-seated sources, because such rocks have never been observed in the surrounding area."

ACKNOWLEDGEMENTS: I wish to thank Professor George KOJIMA of the Hiroshima University for his interst and advice in the progress of the work, and for critical reading of the manuscript. I also wish to thank Mr. Hideo TAKAHASHI of the Hiroshima University for preparation of oriented thin sections for the petrofabric analysis. This study has been supported in part by the Grant in Aid for Scientific Researches from the Ministry of Education, Japan.

II. FABRICS OF PERIDOTITE NODULE

A. MEGASCOPIC FEATURES

The specimen of analysed nodule (HK 63111602) is about 15 cm in diameter Certain planar and linear structures are found in the nodule. These structures seem to be defined mainly by the preferred orientation of grain boundary of olivine as well as by the patterns of preferred location of spinel and pyroxenes in the light olive-green olivine matrix. Grains of orthopyroxene are light brownish-green, and spinel grains are black. There are two or more planar structures intersecting with a common axis. Megascopically, the fabric of the specimen is approximately orthorhombic in symmetry. According to the convention, the fabric axes *a*, *b*, and *c* are megascopically defined as follows:

The surface *ab* is parallel to the most prominent planar structure.

The axis *b* is the intersection of the planar structures.

The axis *c* is normal to *ab*.

Opposite ends of each axis are designated as plus or minus.

Three mutually perpendicular thin sections, which are normal to the axes *a*, *b*, and *c*, were made, designated as *a*, *b*, and *c* sections respectively (Fig. 1 and Plate 16, Fig. 1).

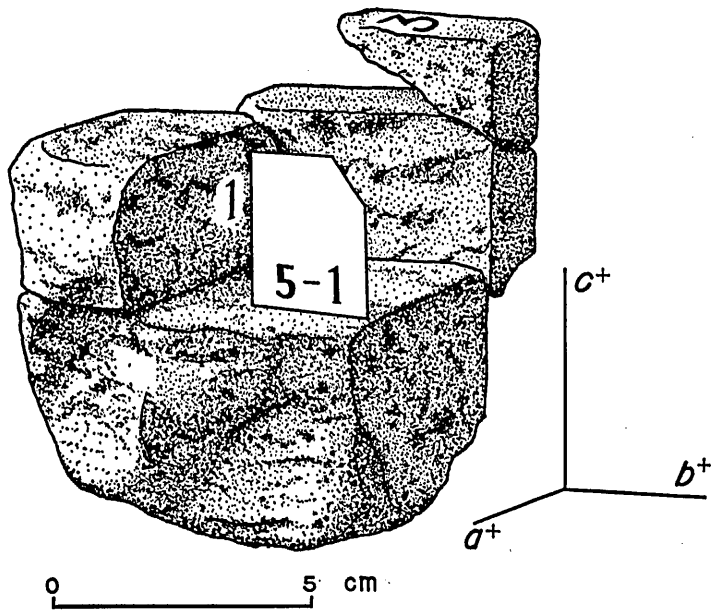

FIG. 1. Sketch showing cut surfaces of the specimen of peridotite nodule (HK 63111602). Fabric axes are selected according to megascopic structures of the nodule. Numbers 5-1, 1, and 3 denote the positions of the *a*, *b*, and *c* sections respectively.

B. MICROSCOPIC FEATURES

The rock is fresh, and consists mostly of inequigranular grains of olivine and orthopyroxene, with small amounts of clinopyroxene and spinel. Olivine predominates over orthopyroxene. Grain of clinopyroxene exists near, coming frequently into contact with, grain of orthopyroxene. Serpentine minerals cannot be found.

1. *Olivine*

Olivine ranges from 0.2 to 5.0mm in grain diameter. In general, the grain boundary is irregular. (010) cleavage is common, and (001) cleavage can be observed in some grains. A system of fracture cleavage is frequently found and the cleavage plane includes [100]. Undulatory extinction bands are frequently seen to develop nearly normal to [100] (Plate 16, Fig. 2). The optic sign of olivine is positive, and the optic axial angle is about 86°.

2. *Orthopyroxene*

Crystal axes of orthopyroxene are named after DEER, HOWIE, and ZUSSMAN (1963). The orthopyroxene ranges from 0.1 to 4.0mm in grain diameter. The mineral possesses prismatic cleavages characteristic of orthopyroxene. Such clinopyroxenes as exsolved cannot be found in the orthopyroxene grains. Deformed grains are frequently observed. In the deformed grains, the angle between two prismatic

cleavages is not constant. It appears that the angle ranges from the original angle to about 60° (Plate 16, Fig. 3). The angle varies within a single grain. It is to be noticed that the deformed grains of orthopyroxene always show a tendency for the (100) plane to bisect the obtuse angle between two prismatic cleavage surfaces. Parting on (010) is common in the deformed grains. In some grains parting on (100) is developed. The optic sign of the orthopyroxene is positive, and the optic axial angle is 78°. The mineral is colorless in thin section, but the deformed grains tend to show weak pleochroism of pale straw-yellow.

3. *Clinopyroxene*

Clinopyroxene ranges from 0.1 to 1.0mm is grain diameter. The grain shape is irregular. Grains of clinopyroxene often contain minute opaque needles that show a tendency to be oriented parallel to a certain definite direction (Plate 16, Fig. 4). The clinopyroxene is colorless in thin section, the extinction angle (c^Z) is about 32°, the optic sign is positive, and the optic axial angle is 62°.

4. *Spinel*

Spinel is opaque in the thin section. Most of the grains show irregular shape. Sometimes the cross-section of regular crystal form is found.

C. Orientation Patterns of Olivine, Orthopyroxene, and Clinopyroxene on the Thin Section

Fabric analysis was carried out on the orientation of olivine, orthopyroxene, and clinopyroxene on the *a*, *b*, and *c* sections. The orientation of crystal grains was determined by measuring the directions of optic elasticity axes X, Y, and Z of each mineral grain. The measured data were plotted on an equal-area projection from the lower hemisphere. Three thin sections used for the fabric analysis are as follows:

a section: GYHK 63111602(5-1)
b section: GYHK 63111602(1)
c section: GYHK 63111602(3)

All the sections were photographed, and the micrographs were enlarged enough in scale to distinguish the smallest grains. Then, every grain in the selected area of each section was measured, numbered, and outlined (Figs. 2, 3, and 4).

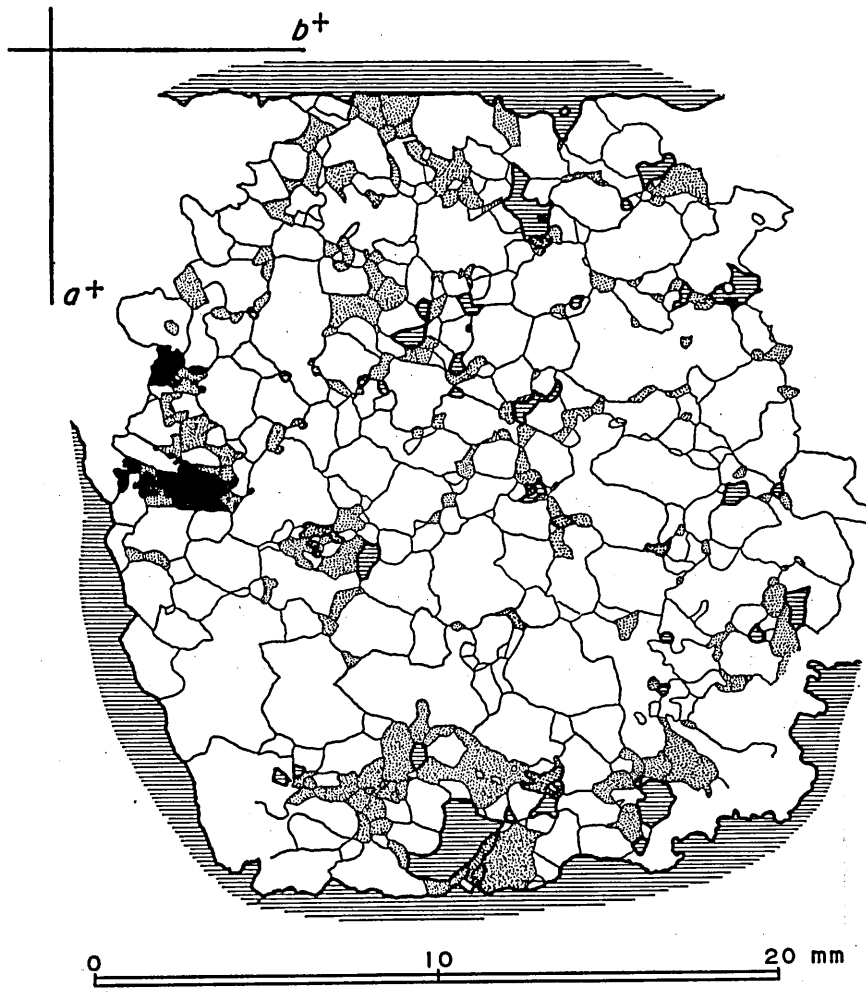

FIG. 2. Tracing of photomicrograph of Section GYHK 63111602(3). Explanation is common to Figs. 2, 3, and 4.

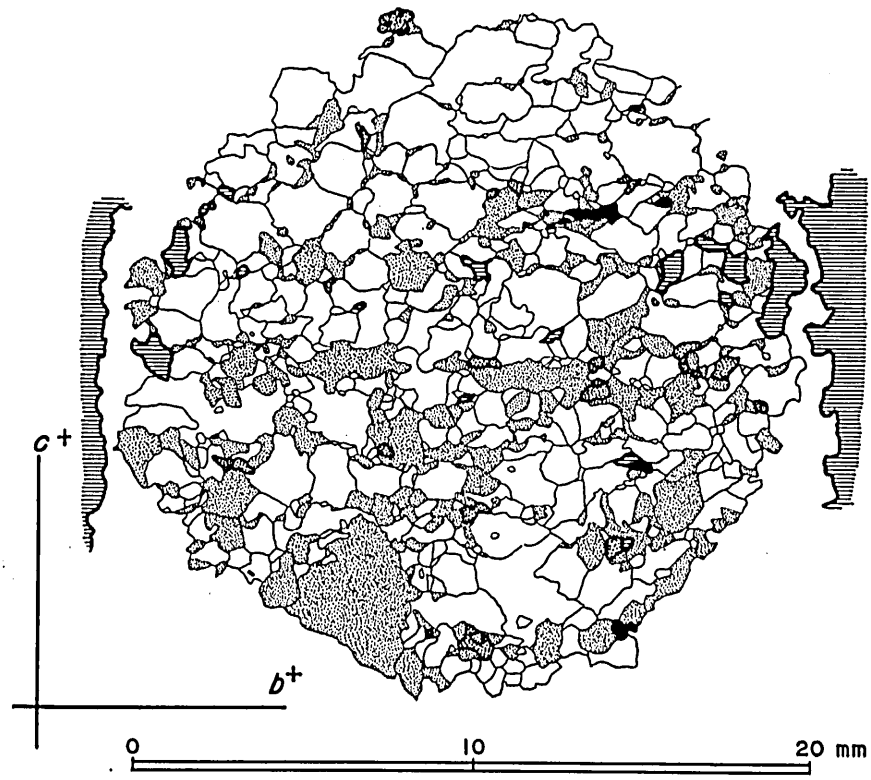

FIG. 3. Tracing of photomicrograph of Section GYHK 63111602(5-1).

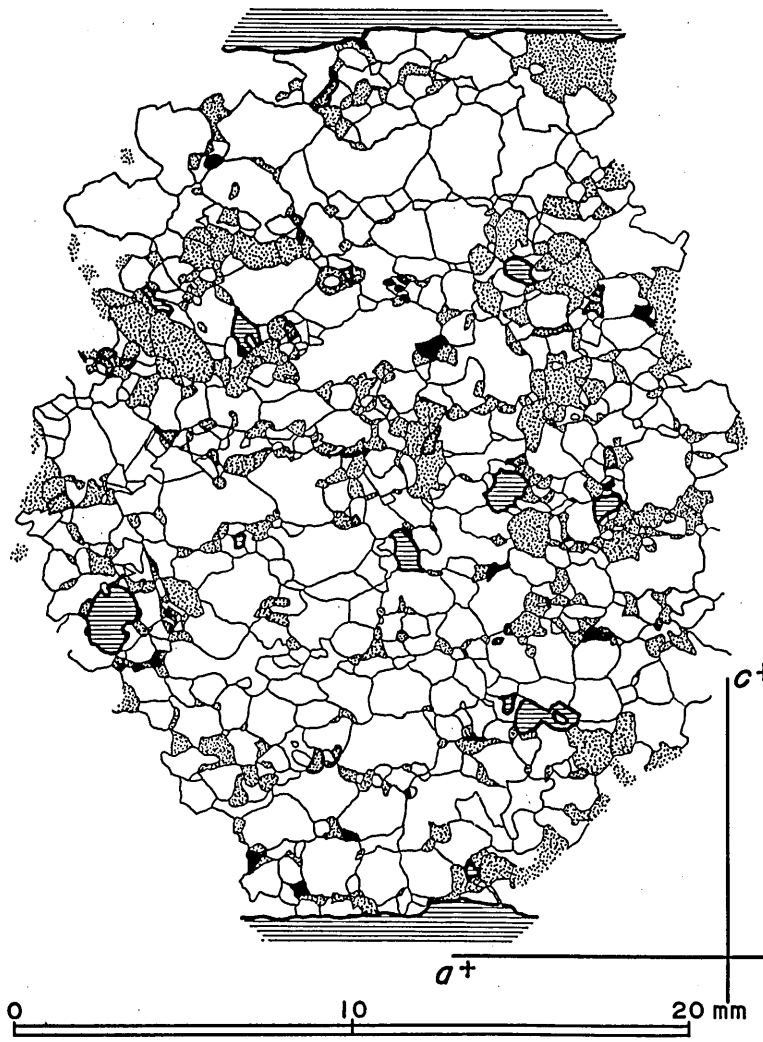

FIG. 4. Tracing of photomicrograph of Section GYHK 63111602(1).

1. *Orientation patterns of olivine, orthopyroxene, and clinopyroxene on the c section*

a. Olivine

Orientation diagrams for X, Y, and Z of 211 olivine grains are shown in Fig. 5a, b, and c. Y shows a remarkable tendency to be concentrated into two areas, each of which consists of separate two or more maxima. The orientation pattern of Y is neither a great circle girdle nor a small circle girdle. It seems that intersecting incomplete girdles are combined in the orientation pattern of Y. Showing a faint tendency to spread along a circle oriented subparallel to *ab*, Z is concentrated subparallel to *b*. X is dispersed within a distinct band oriented subparallel to *ac*.

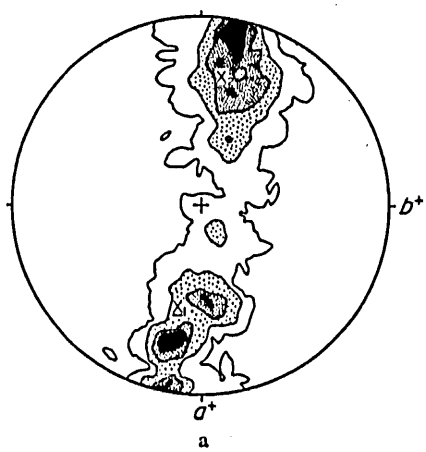

a

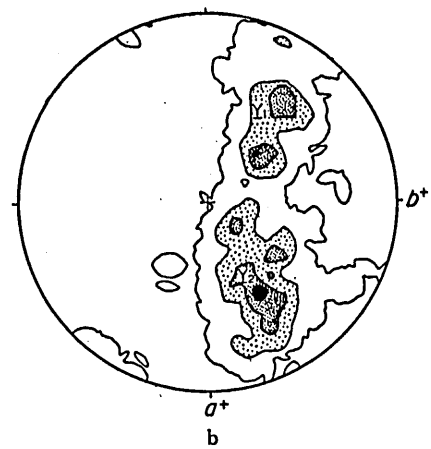

b

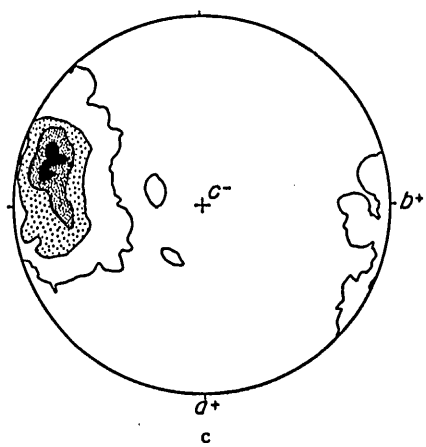

c

FIG. 5. Orientation diagrams for 211 grains of olivine on Section GYHK 63111602(3).
a. Orientation of X. Contours 1-3-5-7% per 1% area.
b. Orientation of Y. Contours 1-3-5-7% per 1% area.
c. Orientation of Z. Contours 1-5-10-15% per 1% area.

There are two major X concentrations, each of which contains two or more separate maxima.

b. Orthopyroxene

Orientation patterns for X, Y, and Z of 167 grains of orthopyroxene are shown in Fig. 6a, b, and c. There is a tendency for X as well as for Z to be concentrated into several separate maxima. The main maxima for X tend to be oriented near *a* and the main maxima for Z near *b*. Y is concentrated into several separate maxima occurring near *c*.

c. Clinopyroxene

The distribution of X, Y, and Z of 9 clinopyroxene grains is shown in Fig. 7a, b, and c.

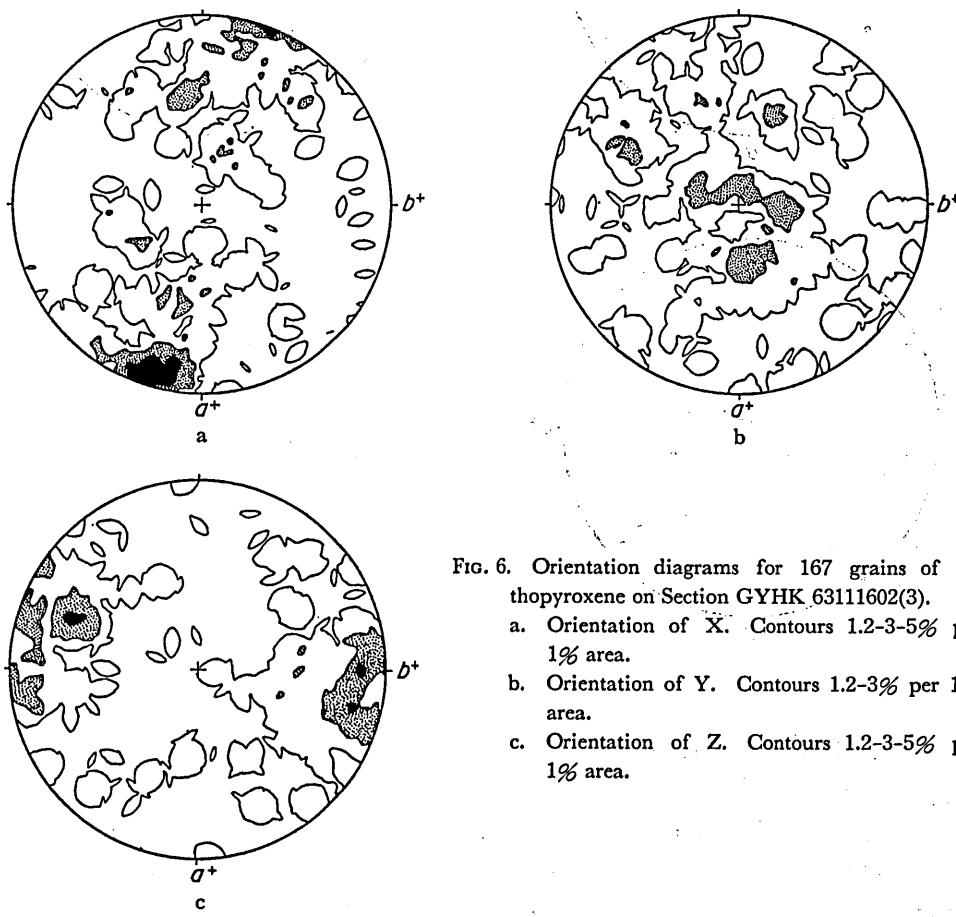

FIG. 6. Orientation diagrams for 167 grains of orthopyroxene on Section GYHK 63111602(3).

a. Orientation of X. Contours 1.2-3-5% per 1% area.

b. Orientation of Y. Contours 1.2-3% per 1% area.

c. Orientation of Z. Contours 1.2-3-5% per 1% area.

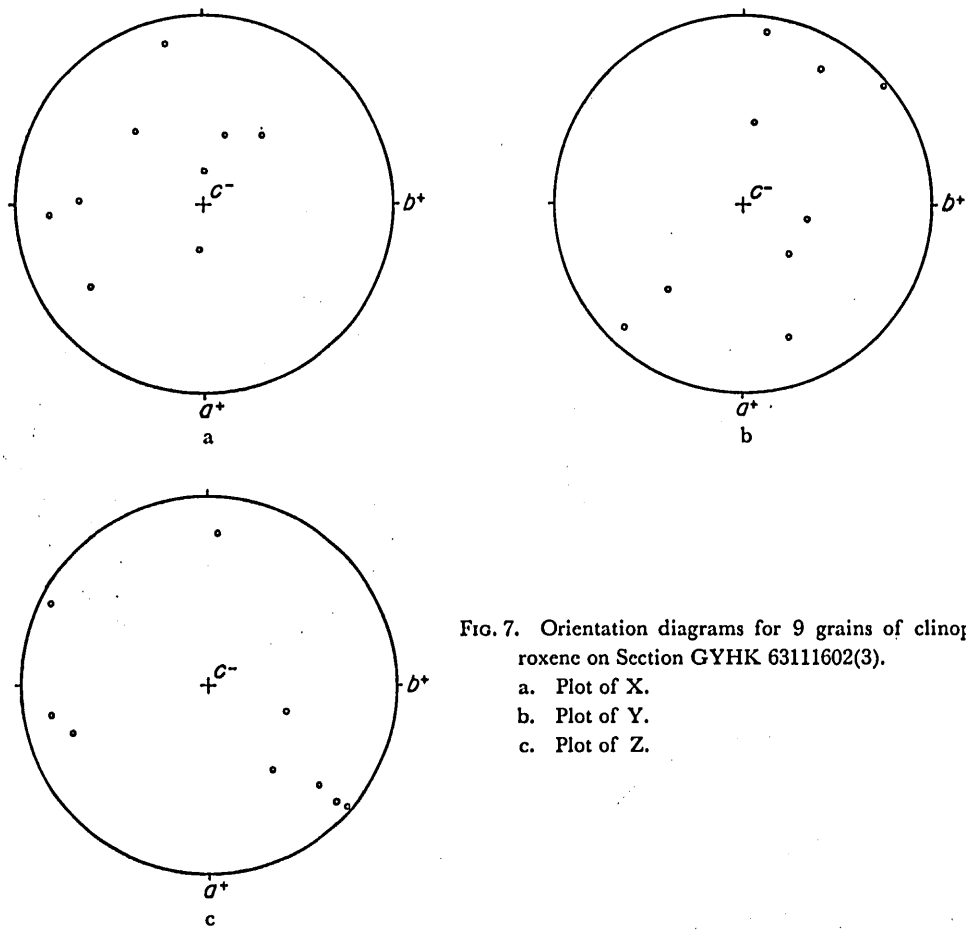

FIG. 7. Orientation diagrams for 9 grains of clinopyroxene on Section GYHK 63111602(3).
a. Plot of X.
b. Plot of Y.
c. Plot of Z.

2. *Orientation patterns of olivine, orthopyroxene, and clinopyroxene on the a section*

a. Olivine

Orientation diagrams for X, Y, and Z of 262 grains of olivine are shown in Fig. 8a, b, and c. Z tends to be concentrated into a single maximum oriented subparallel to *b*. X shows a tendency to be dispersed within a broad band which is roughly perpendicular to *b*. Two major X concentrations occur within the band. Y is distributed within a broad band in which two major Y concentrations occur. It is to be noticed that the band for Y does not coincide in attitude with the band for X.

b. Orthopyroxene

Orientation diagrams for X, Y, and Z of 224 orthopyroxene grains are shown in Fig. 9a, b, and c. X is concentrated into several maxima dispersed in the diagram, and the major concentration occurs near *a*. Z shows a tendency to be concentrated

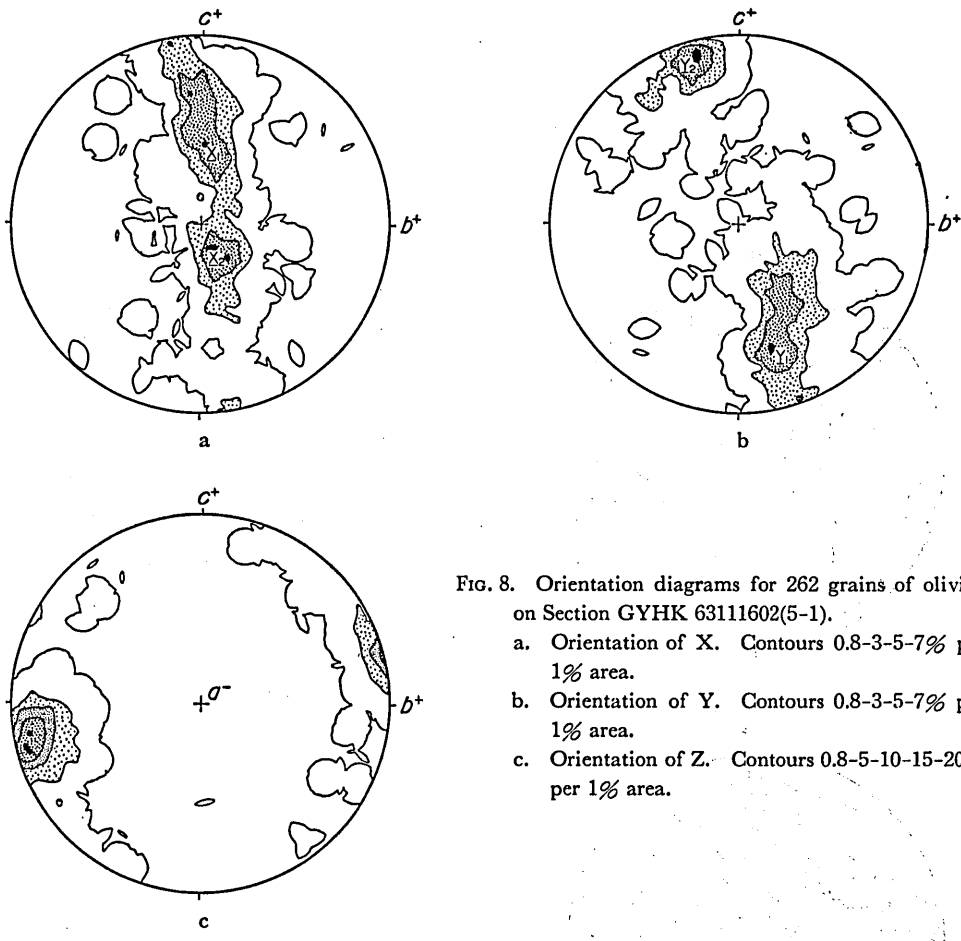

FIG. 8. Orientation diagrams for 262 grains of olivine on Section GYHK 63111602(5-1).
a. Orientation of X. Contours 0.8-3-5-7% per 1% area.
b. Orientation of Y. Contours 0.8-3-5-7% per 1% area.
c. Orientation of Z. Contours 0.8-5-10-15-20% per 1% area.

into several maxima occurring along the great circle *bc*. Though Y is concentrated into several weak maxima, any tendency of preferred orientation for Y cannot be detected.

c. Clinopyroxene

The distribution of X, Y, and Z of 25 clinopyroxene grains is shown in Fig. 10a, b, and c.

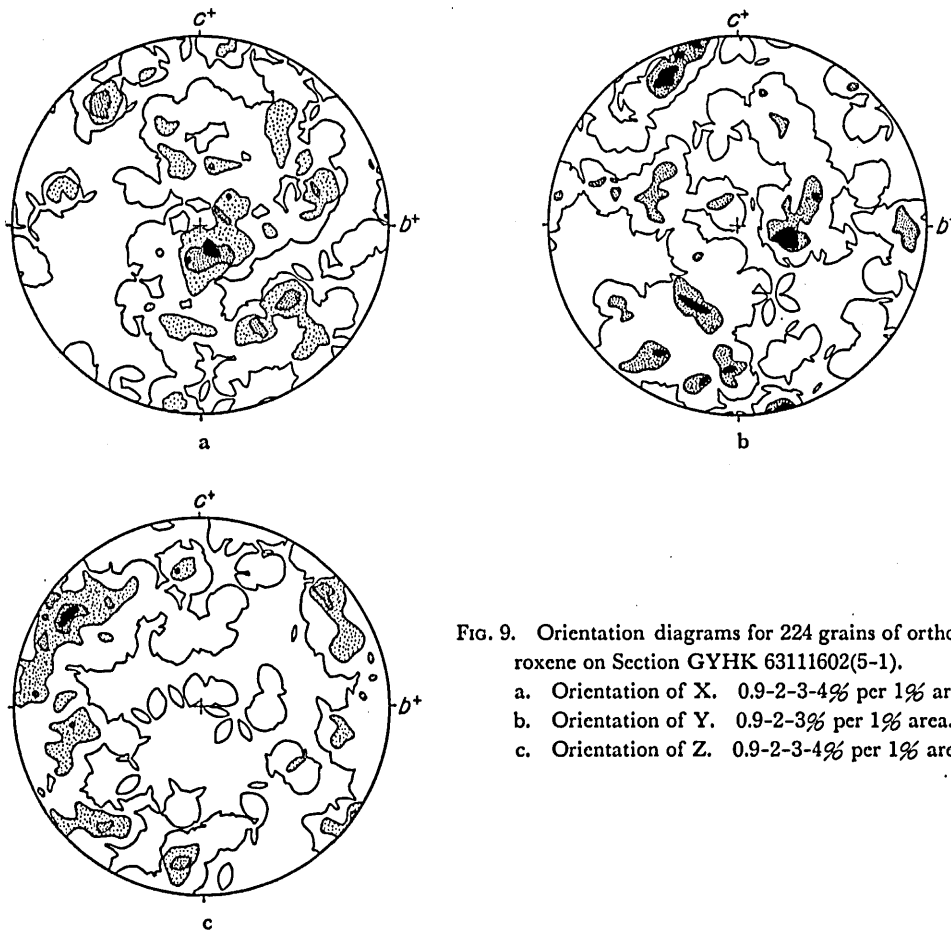

FIG. 9. Orientation diagrams for 224 grains of orthopyroxene on Section GYHK 63111602(5-1).
a. Orientation of X. 0.9-2-3-4% per 1% area.
b. Orientation of Y. 0.9-2-3% per 1% area.
c. Orientation of Z. 0.9-2-3-4% per 1% area.

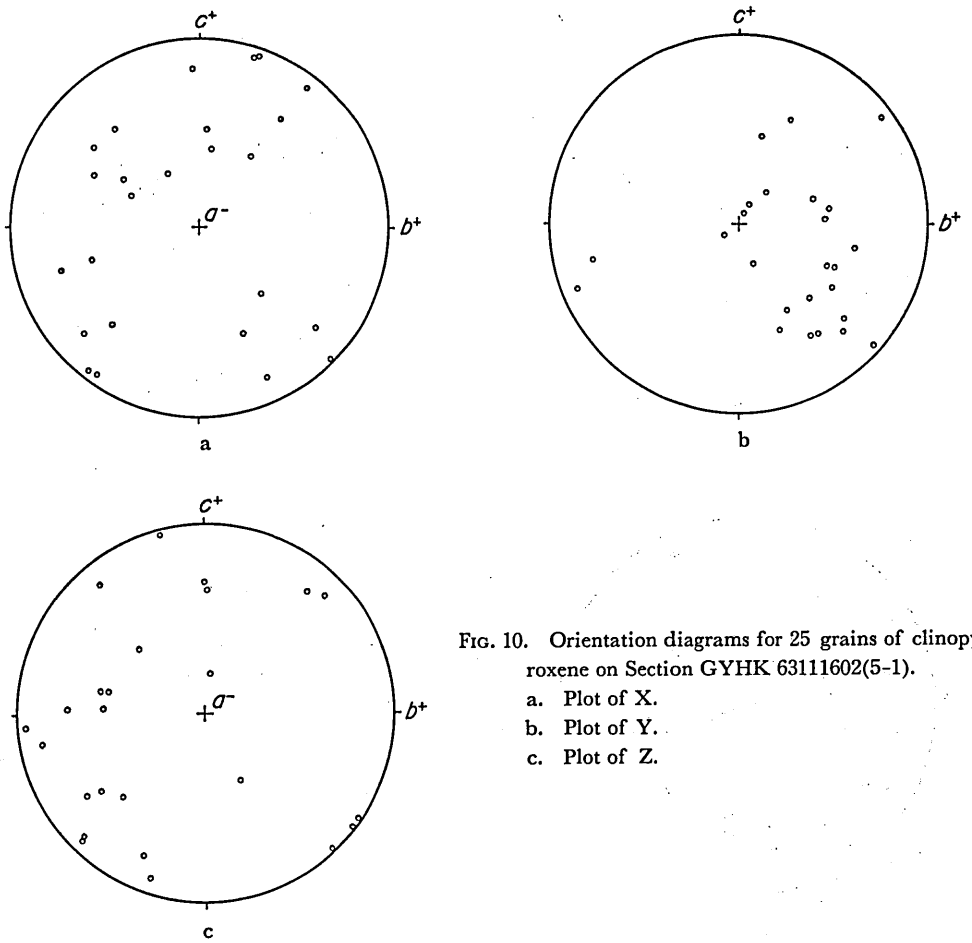

FIG. 10. Orientation diagrams for 25 grains of clinopyroxene on Section GYHK 63111602(5-1).
a. Plot of X.
b. Plot of Y.
c. Plot of Z.

3. *Orientation patterns of olivine, orthopyroxene, and clinopyroxene on the b section*

a. Olivine

Orientation diagrams for X, Y, and Z of 307 olivine grains are shown in Fig. 11a, b, and c. Z shows a distinct tendency to be oriented parallel to *b*. Each of X and Y tends to be distributed within a band subparallel to *ac*. Three major concentrations occur within each band. The orientation pattern for Y may be regarded as a crossed girdle type, in which two or more intersecting girdles are combined.

b. Orthopyroxene

Orientation diagrams for X, Y, and Z of 226 grains of orthopyroxene are shown in Fig. 12a, b, and c. X shows a tendency to be dispersed within a broad band subparallel to *ac*, and the major X concentration within the band occurs near *a*. Z is distributed within a broad girdle subparallel to *bc*, and the major Z concentration occurs near *b*. Although Y is concentrated into several maxima, any tendency of

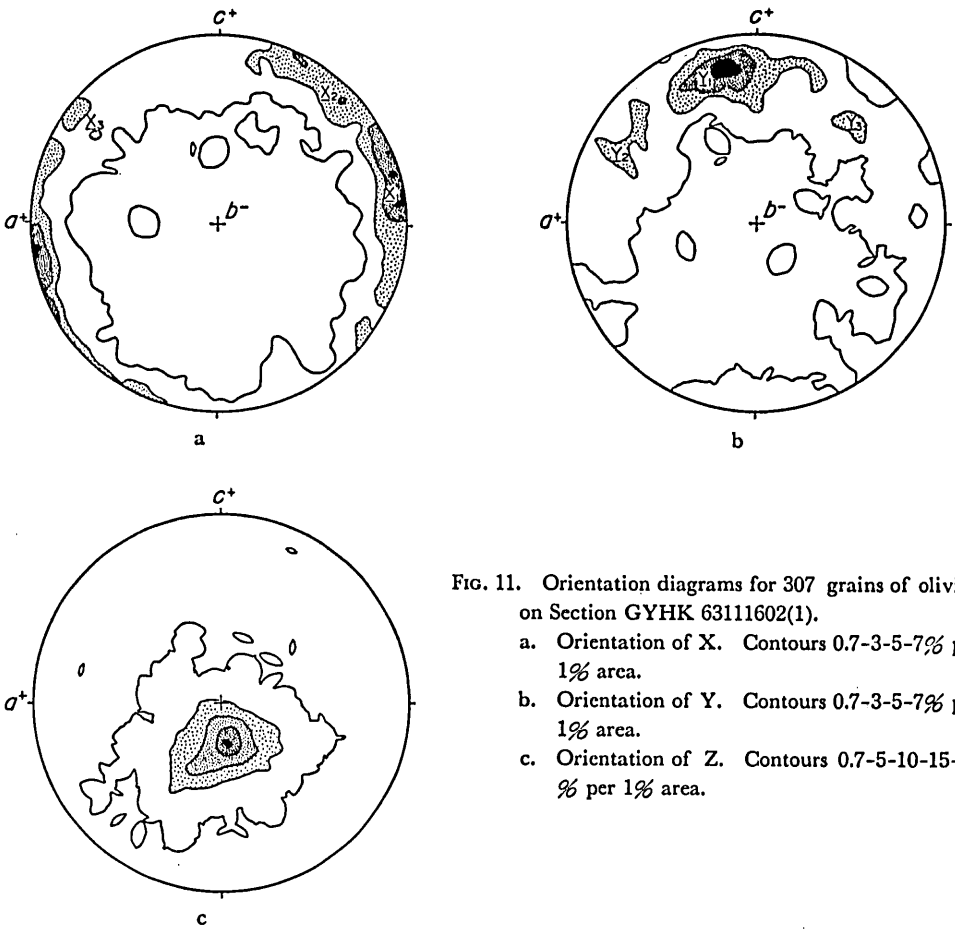

FIG. 11. Orientation diagrams for 307 grains of olivine on Section GYHK 63111602(1).
a. Orientation of X. Contours 0.7-3-5-7% per 1% area.
b. Orientation of Y. Contours 0.7-3-5-7% per 1% area.
c. Orientation of Z. Contours 0.7-5-10-15-18 % per 1% area.

preferred orientation of Y cannot be detected.

c. Clinopyroxene

Orientation diagrams for X, Y, and Z of 29 clinopyroxene grains are shown in Fig. 13a, b, and c. From the diagrams it can be inferred that the crystallographic c-axis of clinopyroxene tends to be oriented subparallel to *b* and the (010) plane subparallel to *bc*.

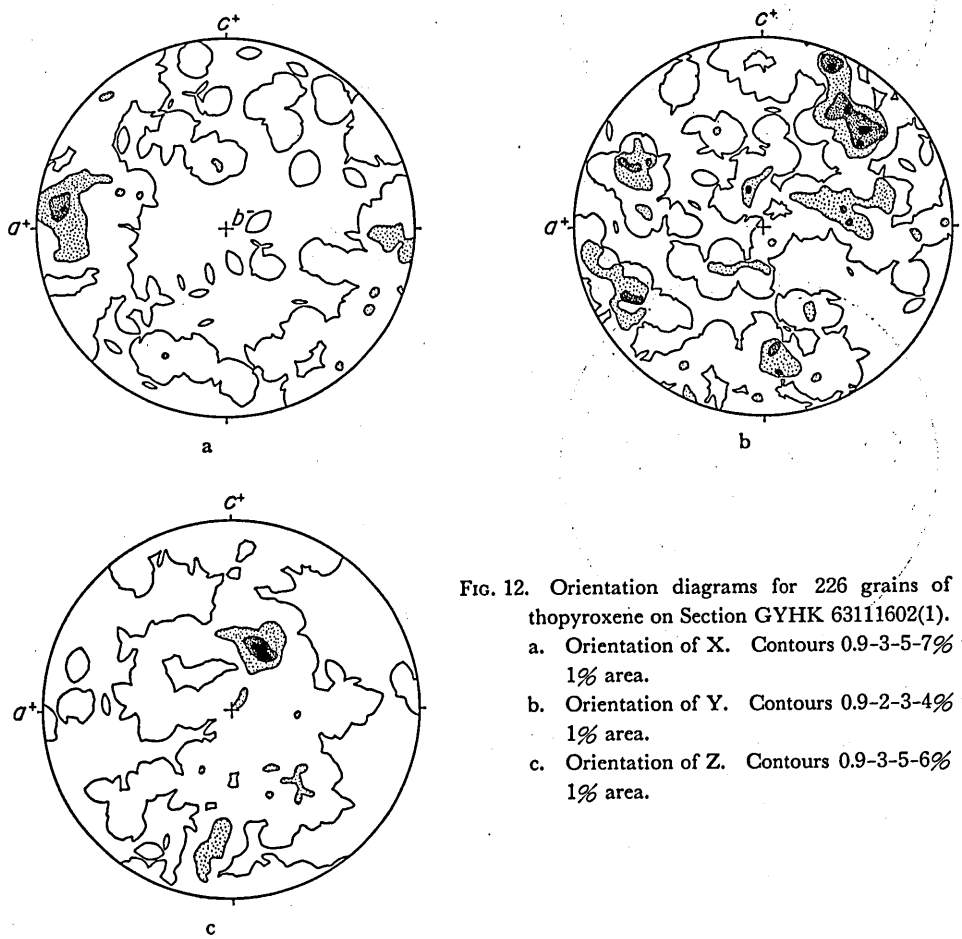

FIG. 12. Orientation diagrams for 226 grains of orthopyroxene on Section GYHK 63111602(1).

a. Orientation of X. Contours 0.9-3-5-7% per 1% area.

b. Orientation of Y. Contours 0.9-2-3-4% per 1% area.

c. Orientation of Z. Contours 0.9-3-5-6% per 1% area.

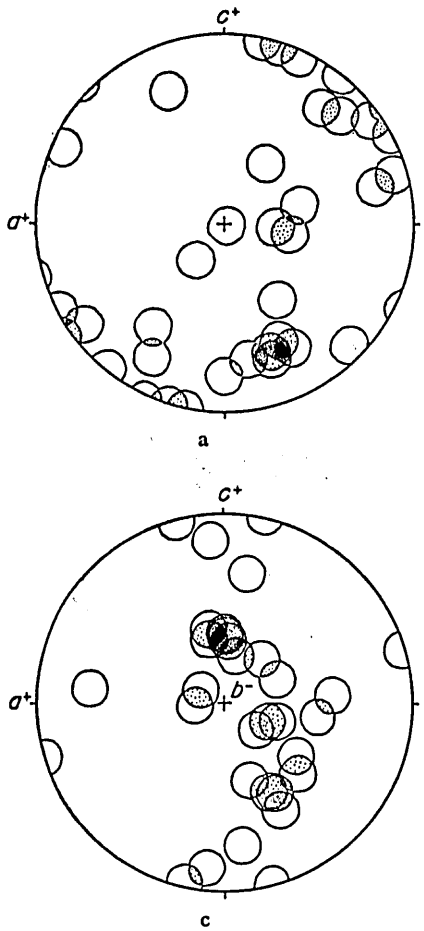

FIG. 13. Orientation diagrams for 29 grains of clinopyroxene on Section GYHK 63111602(1).
a. Orientation of X. Contours 3.4-6.9-10.3-13.8% per 1% area.
b. Orientation of Y. Contours 3.4-6.9-10.3-13.8-17.2% per 1% area.
c. Orientation of Z. Contours 3.4-6.9-10.3-13.8-17.2% per 1% area.

D. OLIVINE, ORTHOPYROXENE, AND CLINOPYROXENE FABRICS IN PERIDOTITE NODULE

1. *Olivine fabric in peridotite nodule*

Judging from the orientation patterns for olivine on these three sections, the nodule is fairly homogeneous with respect to the lattice orientation of olivine. There is a remarkable tendency for Z of olivine to be oriented subparallel to *b*. X and Y of olivine tend to lie on *ac*. Two major X concentrations and two major Y concentrations occur in the olivine orientation diagrams for each of the *a* and *c* sections. In the olivine orientation diagrams for the *b* section occur three major X concentrations and three major Y concentrations. In the olivine orientation diagrams for each section it is found that one of the major X concentrations lies at about 90° to one of the major Y concentrations. In the diagrams for each of the *a* and *c* sections, there are two pairs of such major X and Y concentrations as are about 90° apart. Three pairs occur in the diagrams for the *b* section. Each pair of the

major X and Y concentrations may form an orientation pattern for each of different direction groups of olivine grains. In this connection, the sole Z maximum in the olivine orientation diagrams for each of the *a*, *b*, and *c* sections should be regarded as consisting of two or more Z concentrations corresponding respectively to the orientation patterns for the different direction groups of olivine grains. Accordingly, these pairs of the major X, Y, and Z concentrations in the orientation diagrams of olivine are designated as $\underline{X}_1$, $\underline{Y}_1$, and $\underline{Z}_1$; $\underline{X}_2$, $\underline{Y}_2$, and $\underline{Z}_2$; and $\underline{X}_3$, $\underline{Y}_3$, and $\underline{Z}_3$. In the diagrams for each section, the girdle pattern of X does not coincide in orientation with that of Y, and the girdle pattern of Y, which is more distinct than that of X, seems to be a crossed girdle pattern consisting of two or more intersecting girdles. Then, it seems that the lattice orientation pattern of olivine in the nodule has monoclinic symmetry and the single symmetry plane is subparallel to *bc*. It is likely that the peridotite nodule contains two or more different direction groups of olivine grains.

2. *Orthopyroxene fabric in peridotite nodule*

Judging from the orthopyroxene orientation patterns for the *a*, *b*, and *c* sections, it can be inferred that the lattice orientation of orthopyroxene is rather homogeneous through the nodule. In general, the orthopyroxene shows the tendencies for X to be distributed in a broad band oriented subparallel to *ac* and for Z in a broad band subparallel to *bc*. Major X concentrations occur near *a*, and major Z concentrations near *b*. Although the diagram for Y shows several weak maxima, no preference can be found. The lattice orientation patterns of orthopyroxene suggest that most orthopyroxene grains show the tendencies for the (010) plane to lie on *bc* and for the crystallographic c-axis to be oriented roughly parallel to *b*.

3. *Clinopyroxene fabric in peridotite nodule*

9 orientation data from the *c* section and 25 data from the *a* section are rotated on the *ac* plane, and they are combined with 29 orientation data on the *b* section. Then, the orientation diagrams for X, Y, and Z of 63 clinopyroxene grains are made. They are shown in Fig. 14a, b, and c. Major Y concentrations occur near *a*, and major Z concentrations around *b*. The orientation patterens for both Y and Z of clinopyroxene suggest that the clinopyroxene shows the tendencies for the (010) plane to be oriented parallel to *bc* and for the crystallographic c-axis roughly parallel to *b*.

4. *Mutual geometric relationships of olivine, orthopyroxene, and clinopyroxene fabrics in peridotite nodule*

Orthopyroxene and clinopyroxene show common tendencies for the (010) plane to lie on *bc* and for the crystallographic c-axis to be oriented roughly parallel to *b*. Although in respect to the lattice orientation pattern the clinopyroxene in this nodule has a resemblance to clinopyroxenes described in other tectonites (KOJIMA and HIDE,

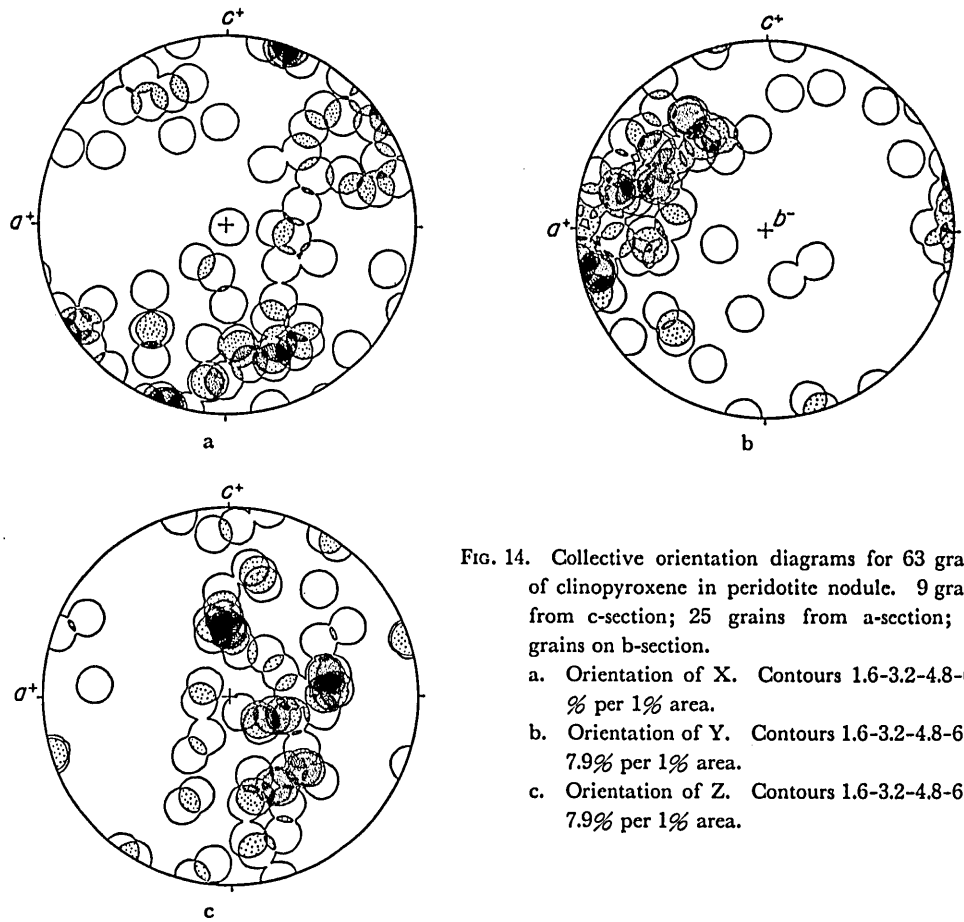

FIG. 14. Collective orientation diagrams for 63 grains of clinopyroxene in peridotite nodule. 9 grains from c-section; 25 grains from a-section; 29 grains on b-section.
a. Orientation of X. Contours 1.6-3.2-4.8-6.3 % per 1% area.
b. Orientation of Y. Contours 1.6-3.2-4.8-6.3-7.9% per 1% area.
c. Orientation of Z. Contours 1.6-3.2-4.8-6.3-7.9% per 1% area.

1957; YOSHINO, 1961, 1964), clinopyroxenes in those tectonites show the tendencies for the (010) plane to be oriented parallel to *ab* and for the crystallographic c-axis parallel to the fabric axis *b*. It may be assumed that a certain *s*-surface oriented subparallel to *bc* and a certain linear structure subparallel to *b* are defined statistically by the lattice orientation patterns of the clinopyroxene and the orthopyroxene in the nodule. Though the linear structure oriented subparallel to *b* may be defined statistically by the lattice orientation patterns of the olivine in the nodule, the fabric defined by the lattice orientation of olivine seems to be incompatible with the fabric defined by the lattice orientation of both pyroxenes in the nodule.

E. AXIAL-DISTRIBUTION-ANALYSIS FOR [001] OF OLIVINE

As mentioned in the preceding pages the nodule seems to consist of two or more different direction groups of olivine grains. Two or more major concentrations occur on each of the orientation diagrams for X and Y of olivine, and more than

one X–Y girdle can be perceived on the orientation diagrams for each of the *a*, *b*, and *c* sections. In general, however, the major concentration areas are more distinct in the Y pattern than the X pattern. Accordingly, spatial distribution of olivine grains belonging to different individual direction groups was examined by the axial-distribution-analysis for Y of olivine.

1. *Axial-distribution-analysis for* [001] *of olivine on the c section*

Two major Y concentrations, designated as $Y_1(c)$ and $Y_2(c)$, occur in the orientation pattern of Y for 211 olivine grains (Fig. 5b). The orientation diagram for Y is divided into three areas representing respective direction groups, designated as $G_1(c)$, $G_2(c)$, and $G_3(c)$. These direction groups are shown in Fig. 15. $G_1(c)$ includes olivine grains whose Y axes lie within a small circle having the radius of 33° at $Y_1(c)$, and $G_2(c)$ those with Y axes within a small circle having the radius of 33° at $Y_2(c)$. The number of grains belonging to each of these direction groups is as follows:

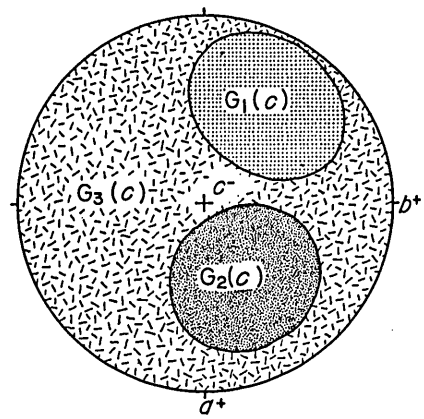

FIG. 15. Division of Fig. 5b into three direction groups.

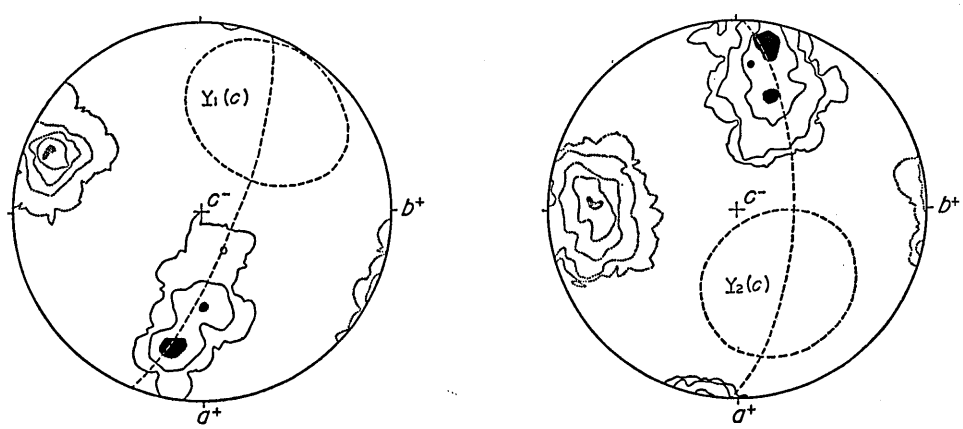

FIG. 16. Orientation diagrams for olivine grains belonging to the individual direction groups, $G_1(c)$ and $G_2(c)$, on Section GYHK 63111602(3). Broken great circle is drawn perpendicular to the center of Z maximum.

a. Orientation diagram for 74 grains belonging to $G_1(c)$.
Contours: X, 2.7-10-20% (full lines); Z, 2.7-10-20-30-40% (dotted lines).

b. Orientation diagram for 100 grains belonging to $G_2(c)$.
Contours: X, 2-5-10-15% (full lines); Z, 2-5-10-15-20% (dotted lines).

$G_1(c)$ 74
$G_2(c)$ 100
$G_3(c)$ 37

The diagrams for $G_1(c)$ and $G_2(c)$ are shown in Fig. 16a and b. Each diagram contains both the orientation patterns for X and Z. There is a distinct tendency for Z to be concentrated into a single maximum. X is also concentrated into a distinct area. In these diagrams, respective Y orientation areas for the two groups, $G_1(c)$ and $G_2(c)$, are represented by broken small circles, that is, $\underline{Y}_1(c)$ and $\underline{Y}_2(c)$, and each broken great circle is drawn perpendicular to the center of the Z maximum. Two areas of X concentration for the groups, $G_1(c)$ and $G_2(c)$, coincide respectively with two major X concentrations, $\underline{X}_1(c)$ and $\underline{X}_2(c)$, in the collective diagram for 211

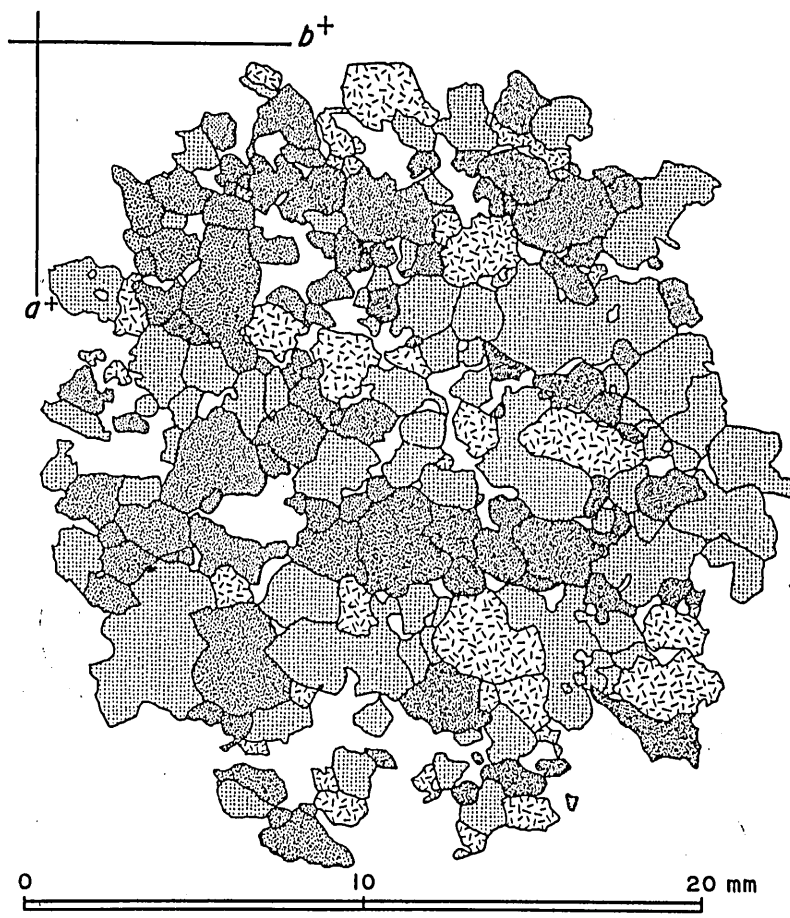

FIG. 17. Axial distribution diagram for olivine on Section GYHK 63111602(3). Each grain is shaded to correspond to one of the direction groups of Fig. 15.

olivine grains (Fig. 5a). Two Z maxima for the groups, $G_1(c)$ and $G_2(c)$, must correspond with the supposed Z concentrations, $\underline{Z}_1(c)$ and $\underline{Z}_2(c)$, respectively. The center of the Z maximum for the group $G_1(c)$ and that for the group $G_2(c)$ are about 23° apart. Spatial distribution of olivine grains belonging to the individual direction groups, $G_1(c)$, $G_2(c)$, and $G_3(c)$, on the *c* section is shown in Fig. 17. Each grain is shaded to correspond to one of the direction groups in Fig. 15. Fig. 17 brings out the tendency for the olivine grains belonging to each of the direction groups, $G_1(c)$ and $G_2(c)$, to be mutually associated in somewhat laminated domain.

2. *Axial-distribution-analysis for* [001] *of olivine on the a section*

The orientation pattern for Y of 262 olivine grains has two major Y concentrations, that is, $\underline{Y}_1(a)$ and $\underline{Y}_2(a)$ (Fig. 8b). The pattern is arbitrarily divided into three areas, each representing respective direction groups, namely, $G_1(a)$, $G_2(a)$, and $G_3(a)$ (Fig. 18). $G_1(a)$ contains olivine grains whose Y axes are oriented within a small circle having the radius of 25° at $\underline{Y}_1(a)$, and $G_2(a)$ those with Y axes within a small circle having the radius of 17° at $\underline{Y}_2(a)$. The number of grains belonging to the respective direction groups is as follows:

$G_1(a)$	83
$G_2(a)$	40
$G_3(a)$	139

The orientation diagrams for the respective direction groups, $G_1(a)$ and $G_2(a)$, are shown in Fig. 19a and b. Each diagram consists of orientation patterns for both X and Z. In these diagrams, there is a tendency for each of X and Z to be concentrated into a single maximum. Orientation areas of Y for the direction groups $G_1(a)$ and $G_2(a)$ are represented respectively by broken small circles $\underline{Y}_1(a)$ and $\underline{Y}_2(a)$, and each broken great circle is drawn perpendicular to the center of the Z maximum. Two X maxima for the groups $G_1(a)$ and $G_2(a)$ coincide respectively with two major

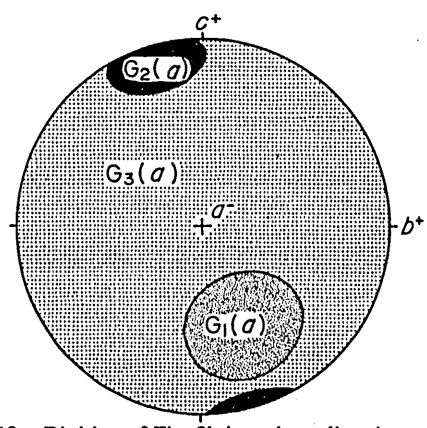

Fig. 18. Division of Fig. 8b into three direction groups.

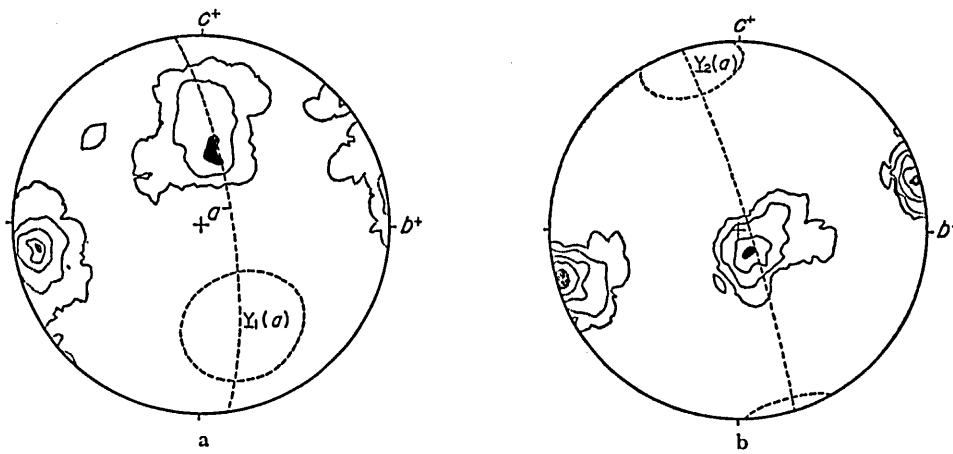

FIG. 19. Orientation diagrams for olivine grains belonging to the individual direction groups, $G_1(a)$ and $G_2(a)$, on Section GYHK 63111602(5-1). Broken great circle is drawn perpendicular to the center of Z maximum.

a. Orientation diagram for 83 grains belonging to $G_1(a)$.
Contours: X, 2.4-10-20% (full lines); Z, 2.4-10-20-30-37% (dotted lines).

b. Orientation diagram for 40 grains belonging to $G_2(a)$.
Contours: X, 5-15-25-35% (full lines); Z, 5-10-20-30-40% (dotted lines).

X concentrations $\underline{X}_1(a)$ and $\underline{X}_2(a)$ in the collective diagram for 262 olivine grains (Fig. 8a). Z maxima for the groups $G_1(a)$ and $G_2(a)$ must correspond to the supposed Z concentrations $\underline{Z}_1(a)$ and $\underline{Z}_2(a)$ respectively. The center of the Z maximum for the group $G_1(a)$ and that for the group $G_2(a)$ are about 13° apart. Spatial distribution of olivine grains belonging to the individual direction groups, $G_1(a)$, $G_2(a)$, and $G_3(a)$, on the *a* section is shown in Fig. 20. Each grain is shaded to correspound to one of the direction groups of Fig. 18. It is readily seen that the olivine grains belonging to the individual direction groups show the tendency to be mutually associated in somewhat laminated domain developed subparallel to *b*.

3. *Axial-distribution-analysis for* [001] *of olivine on the b section*

Three major Y concentrations, designated as $\underline{Y}_1(b)$, $\underline{Y}_2(b)$, and $\underline{Y}_3(b)$, occur in the orientation pattern for Y of 307 olivine grains (Fig. 11b). As shown in the preceding pages, two or more girdles can be detected to be combined in the fabric pattern for Y. First, the orientation patterns for X and Z of olivine which has Y concentrated into each of $\underline{Y}_1(b)$, $\underline{Y}_2(b)$, and $\underline{Y}_3(b)$ are examined. The major Y concentrations in Fig. 11b are arbitrarily divided into three areas representing respective direction groups, I, II, and III, as shown in Fig. 21. Group I contains olivine grains whose Y axes lie within a small circle having the radius of 25° at $\underline{Y}_1(b)$. Group II includes grains whose Y axes lie in the elongated area II, and group III those with Y axes in the elongated area III in Fig. 21. The number of grains belonging to the

respective direction groups is as follows:

Group I	98
Group II	54
Group III	51

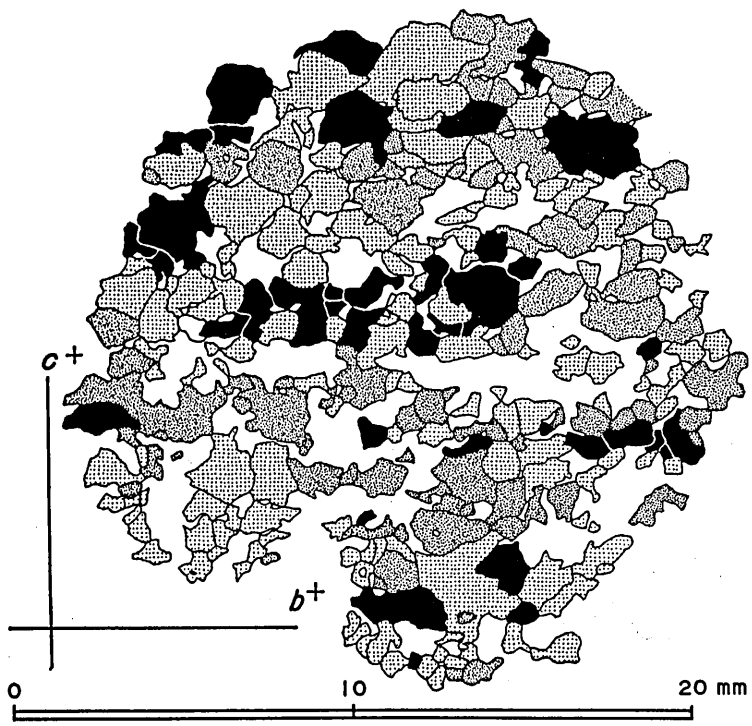

FIG. 20. Axial distribution diagram for olivine on Section GYHK 63111602(5-1). Each grain is shaded to correspond to one of the direction groups of Fig. 18.

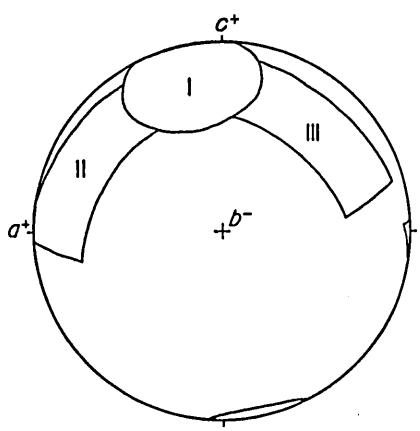

FIG. 21. Division of Y maxima of Fig. 11b into three direction groups.

Three composite orientation diagrams for these three direction groups, I, II, and III, are shown in Fig. 22a, b, and c. There can be seen tendencies for Z to be concentrated into a distinct single maximum and for X to be distributed in somewhat elongated area. That is common to all the diagrams for groups I, II, and III. In these diagrams, the orientation areas for Y with respect to the different direction groups, I, II, and III, are represented by $\underline{Y}_1(b)$, $\underline{Y}_2(b)$, and $\underline{Y}_3(b)$, respectively. Three X maxima for groups I, II, and III correspond respectively to three major X concentrations, $\underline{X}_1(b)$, $\underline{X}_2(b)$, and $\underline{X}_3(b)$, in the collective diagram for X of 307 olivine grains. Three Z maxima for these three groups, I, II, and III, must correspond to the supposed Z concentrations, $\underline{Z}_1(b)$, $\underline{Z}_2(b)$, and $\underline{Z}_3(b)$, respectively. The center of Z maximum for group II and that for group III are about 25° apart. The center of Z maximum for group I lies between them. It is to be noticed that three well-defined Z maxima for groups I, II, and III tend to lie on the surface subparallel to *ab*.

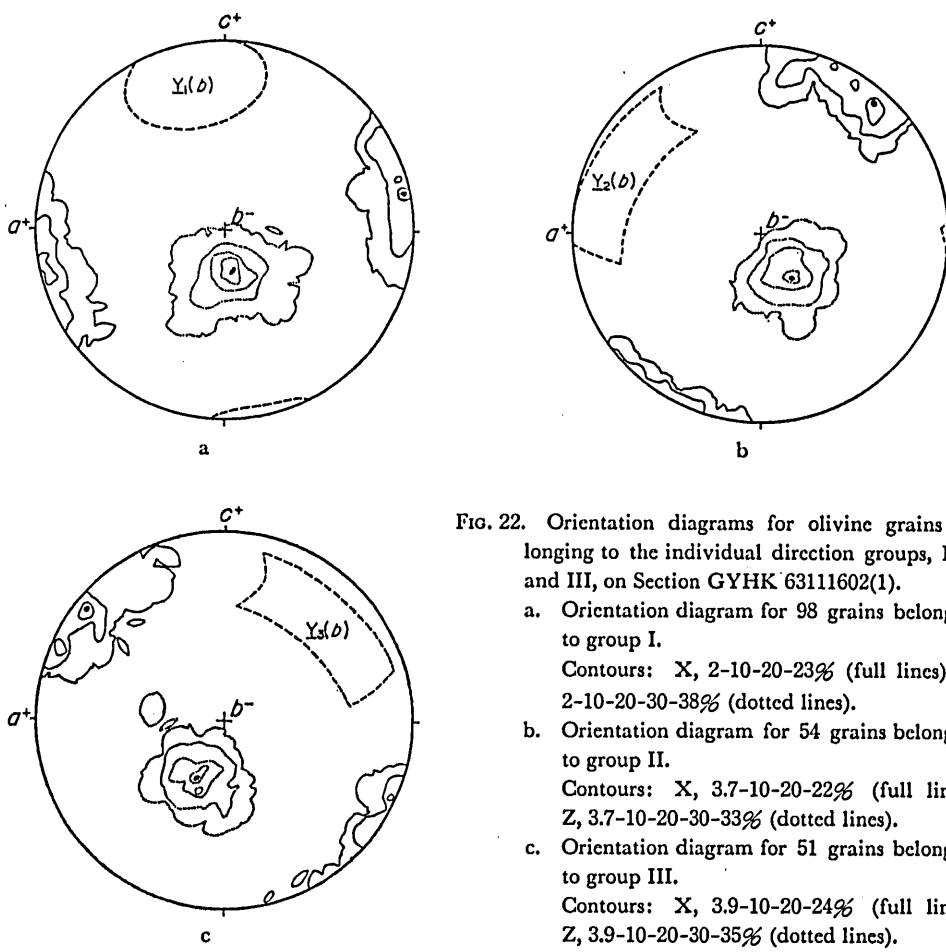

FIG. 22. Orientation diagrams for olivine grains belonging to the individual direction groups, I, II, and III, on Section GYHK 63111602(1).

a. Orientation diagram for 98 grains belonging to group I.
Contours: X, 2-10-20-23% (full lines); Z, 2-10-20-30-38% (dotted lines).

b. Orientation diagram for 54 grains belonging to group II.
Contours: X, 3.7-10-20-22% (full lines); Z, 3.7-10-20-30-33% (dotted lines).

c. Orientation diagram for 51 grains belonging to group III.
Contours: X, 3.9-10-20-24% (full lines); Z, 3.9-10-20-30-35% (dotted lines).

The lattice orientation pattern for each of the groups I, II, and III has orthorhombic symmetry. The symmetry of the total orientation patterns for olivine grains on the *b* section is monoclinic, and the single symmetry plane is oriented subparallel to *bc*.

Then, the orientation diagram for Y axes of 307 olivine grains on the *b* section is arbitrarily divided into four areas representing different direction groups, $G_1(b)$, $G_2(b)$, $G_3(b)$, and $G_4(b)$, as shown in Fig. 23. The number of grains belonging to the respective direction groups is as follows:

$G_1(b)$	105
$G_2(b)$	81
$G_3(b)$	60
$G_4(b)$	61

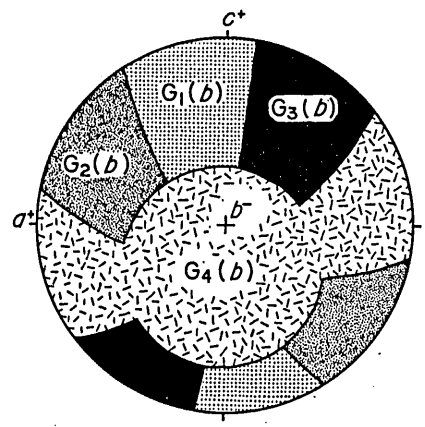

FIG. 23. Division of Fig. 11b into four direction groups.

The spatial distribution of olivine grains belonging to the individual direction groups is shown in Fig. 24. Each grain is shaded to correspond to one of the direction groups.

Every part of olivine domains in the nodule is composed, in general, of two or three different direction groups. Although the symmetry of the total lattice orientation pattern of olivine in the nodule is monoclinic, the olivine grains belonging to the individual direction groups tend to show the preferred orientation of orthorhombic symmetry and to be mutually associated in somewhat laminated domains in the nodule. Occurring close to *b*, the concentration of Z for the individual direction groups tends to disperse on the surface subparallel to *ab*.

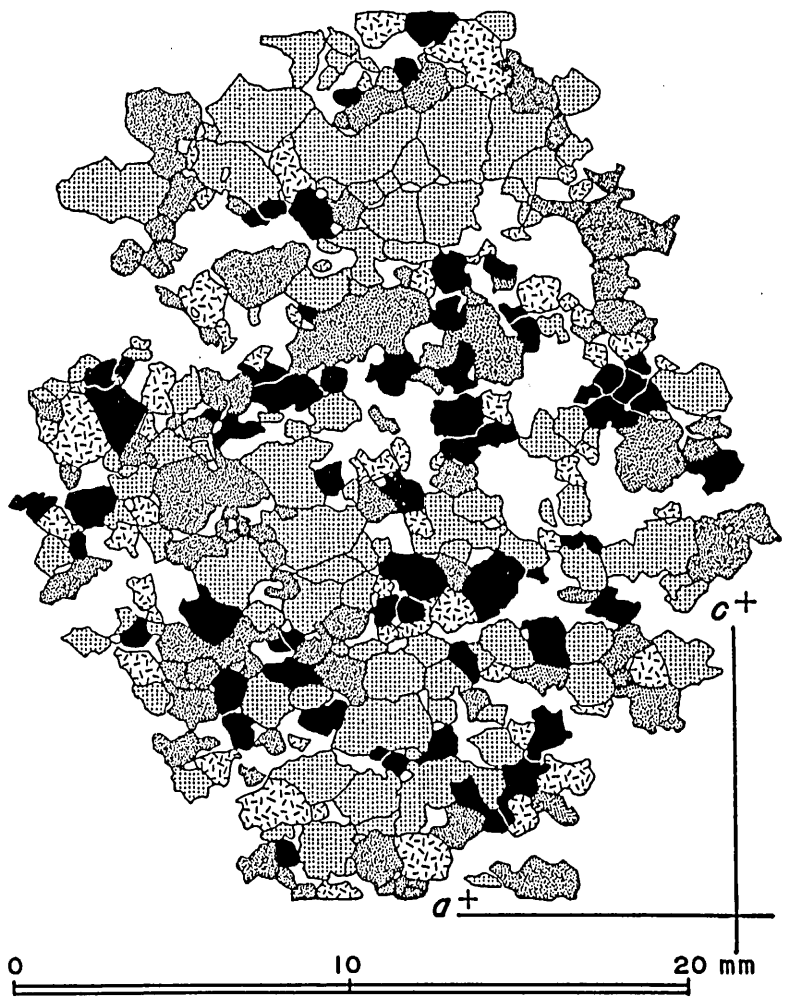

FIG. 24. Axial distribution diagram for olivine on Section GYHK 63111602(1) Grains are shaded to correspond to the orientations similarly shaded in Fig. 23.

III. Evolution of the Fabric

Enstatite tends to occur as aggregates in the olive-green olivine matrix of the nodule. Spatial distribution of the enstatite aggregates was examined on the cut surfaces parallel to *ab*, *bc*, and *ac* of the specimen (Plate 17). On the faces *ab* and *bc*, locally concentrated aggregates of enstatite grains tend to run parallel to *b*, forming irregular shapes. Some of the enstatite aggregates form sharply outlined streaks running parallel to *b*. Elongated domains of enstatite grains are locally bent by indistinctly laminated strain-slip structure intersecting *a*, *b*, and *c* obliquely, and are frequently cut by the slip surfaces. The pattern of distribution of enstatite aggregates on the face *ac* is rather complicated. Though scarcely lengthened, dark colored fine streaks of enstatite aggregates can be seen in places to run parallel to *a* on this face. The enstatite aggregates tend to form groups of indefinite bands which are extended nearly perpendicular to the face *ac*. In such groups can be seen several elongate aggregates arranged zigzag. Some of the folded aggregates seem to be connected. Such megascopic features on the faces *ab*, *bc*, and *ac* are well correlated with the microscopic features on the *c*, *a*, and *b* sections.

The pattern of spatial distribution of enstatite grains is conformable with that of olivine grains belonging to the different individual direction groups and with the pattern of preferred orientation of grain boundaries of olivine. These patterns reveal several *s*-surfaces; namely, the surface S_L defined by the banding of local concentration of enstatite grains, the surface S_1 coinciding with *ab*, the conjugate surfaces, S_2 and S_3, symmetrically inclined to *bc*, and the surface S_4 intersecting obliquely *a*, *b*, and *c* (Fig. 25). The surface S_1 seems to intersect such an earlier foliation S_L as is defined by compositional layering. The conjugate *s*-surfaces, S_2 and S_3, may cut S_1. S_4 showing features of laminated strain-slip structure may be younger than S_2 and S_3. The enstatite aggregates as observed now in the nodule appear to be segments of disrupted laminae which have originated from enstatite-rich layers. It can be seen that S_L, S_1, and the conjugate surfaces, S_2 and S_3, intersect one another in the common axis coinciding with *b*. The three major Y concentrations, $\underline{Y}_1(b)$, $\underline{Y}_2(b)$, and $\underline{Y}_3(b)$, observed in the lattice orientation patterns of olivine on the *b* section seem to be related to S_1, S_2, and S_3 respectively. On the *b* section, S_1 can be correlated with the preferred lattice orientation of the olivine grains belonging to the group I. The preferred lattice orientation of the olivine grains belonging to the group II and that of the olivine

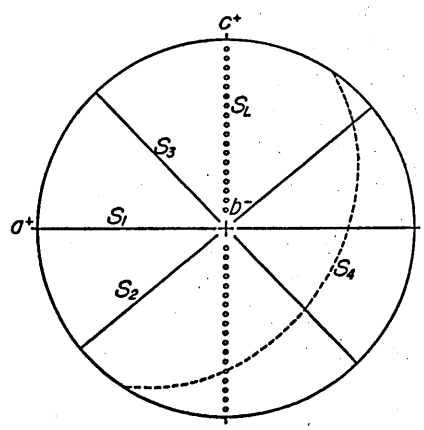

Fig. 25. Five planar structures in peridotite nodule.

grains belonging to the group III on the *b* section can be regarded as related to S_2 and S_3 respectively. The two major Y concentrations in the orientation patterns of olivine for each of the *a* and *c* sections can be regarded as related to any of S_1, S_2, and S_3. Judging from the observed state of preferred lattice orientation of olivine grains, the olivine grains in the nodule seem to show the tendency for the (001) plane to be oriented subparallel to *s*-surface, the development of which is closely related to the development of the preferred lattice orientation of those grains.

The single concentration of [100], in the total orientation pattern of olivine grains, coincides nearly with *b*, that appearing to define the statistical linear structure subparallel to *b*. The [100] maximum in the olivine orientation pattern for the individual direction group tends to disperse on the surface subparallel to *ab*. That may define a statistical *s*-surface subparallel to *ab*. BROTHERS (1959, 1964) discussed the fabric patterns developed from crystal orientation of early formed olivine grains by magma flow. Such structures as have been imposed upon the Ichinomegata peridotite nodule appear unlikely to have resulted from rotation of inequant crystals during gravity settling in magma, but it is highly probable that such fabrics as S_1, S_2, S_3, and S_4 observed in the Ichinomegata peridotite nodule have been evolved through deformation and recrystallization in a solid state. S_1, S_2, S_3, and S_4 may have been formed during a single broad phase of deformation.

As mentioned in the preceding pages, the fabrics of orthopyroxene and clinopyroxene in the nodule are inconsistent with the olivine fabric. A statistical *s*-surface, coinciding roughly with *bc*, seems to be defined by the observed preferred orientation of both pyroxenes. Most of the orthopyroxene grains have been distorted, but such distorted features can scarsely be found in olivine grains. From the consideration of the character of preferred orientation of both pyroxenes and the spatial distribution of orthopyroxene aggregates in the nodule, such a statistical *s*-surface as is defined by the preferred orientation of both pyroxenes seems to be an inherited structure. The statistical *s*-surface defined by the preferred orientation of (010) of each pyroxene may have coincided with S_L defined by the compositional layering. It is likely that S_1 coinciding with *ab* intersected S_L nearly at right angles. It is conceivable that the earlier state of preferred orientation of (010) of each pyroxene has hardly been obliterated through the deformation by which such fabrics as S_1, S_2, S_3, and S_4 have been imposed on the peridotite nodule. The crystallographic c-axis of each pyroxene may have been oriented parallel to a definite direction on S_L.

Concerned with the pattern of movement in the deformation, the olivine fabrics will be examined again in detail. The consistent preference in the lattice orientation pattern of olivine grains belonging to every direction group is represented by orthorhombic symmetry, but the symmetry of the total orientation pattern for all the olivine grains in the nodule is monoclinic. The single plane of symmetry is subparallel to *bc*. Strictly speaking, if the lattice orientation patterns for olivine are

considered with reference to the S_1, S_2, and S_3 structures, the total fabric of olivine of the nodule must be regarded as triclinic. This triclinic feature can well be seen on the b section. The three major [001] concentrations, $\underline{Y}_1(b)$, $\underline{Y}_2(b)$, and $\underline{Y}_3(b)$, in the orientation pattern for Y of olivine on the b section seem to have occurred through the deformation involving the development of the S_1, S_2, and S_3 structures, and three statistical s-surfaces may be also defined by the preferred orientation of the (001) plane of olivine. Such statistical s-surfaces do not always coincide with the planar s-surfaces defined by the preferred location of olivine grains belonging to each direction group as well as by the grain boundary fabric of olivine. Centers of $\underline{Y}_1(b)$, $\underline{Y}_2(b)$, and $\underline{Y}_3(b)$ in the orientation patterns for olivine on the b section deviate from the poles of S_1, S_2, and S_3 respectively. Therefore, designated as S_1', S_2', and S_3', three statistical s-surfaces which are respectively normal to the centers of $\underline{Y}_1(b)$, $\underline{Y}_2(b)$, and $\underline{Y}_3(b)$ are defined. With reference to a, b, and c, the two sets of the s-surfaces are shown in Fig. 26. It is shown that the statistical s-surfaces, S_1', S_2', and S_3', must be rotated clockwise through the angles of 22°, 31°, and 27° about the axes, R_1, R_2, and R_3, respectively, to bring them into coincidence with the planar structures, S_1, S_2, and S_3. While the set of S_1, S_2, and S_3 has orthorhombic symmetry, the set of S_1', S_2', and S_3' has monoclinic symmetry. The lattice orientation patterns of olivine on the b section have a single symmetry plane perpendicular to the center of $\underline{X}_1(b)$. Judging from the close geometrical relationship between the set of S_1, S_2, and S_3, and the set of S_1', S_2', and S_3' on the b section, the triclinic symmetry of the olivine fabrics in the nodule cannot be infered to imply asymmetric overprinting of one set of s-surfaces upon the other set of s-surfaces. Development of triclinic tectonites was discussed by KOJIMA and HIDE (1958), and TURNER and WEISS (1963). The movement picture in the evolution of olivine fabrics of the Ichinomegata peridotite nodule seems to include at least two components; one is the orthorhombic movement picture reflected on the preferred location of the olivine grains belonging to the different individual direction groups as well as on the grain boundary fabrics of olivine, and the other is the monoclinic movement picture reflected on the preferred lattice orientation of olivine.

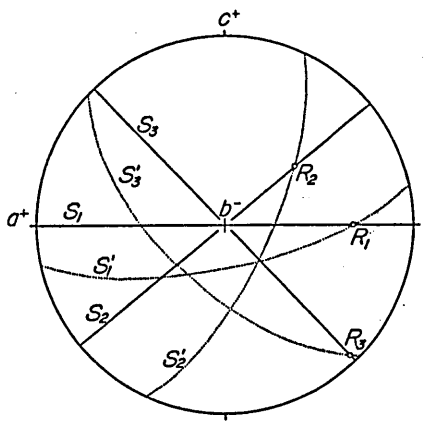

FIG. 26. Two sets of s-surfaces in peridotite nodule.

A number of orientation diagrams for minerals of peridotite nodules as well as those of peridotites of other geologic settings have been recorded, and orienting processes of peridotite minerals have been discussed (ERNST, 1935, 1967; TURNER, 1942; FAIRBAIRN, 1949; PAULITSCH, 1953; LADURNER, 1954; BATTEY, 1960; YOSHINO, 1961, 1964; COLLÉE, 1962; AVE'LALLEMANT, 1967; LAPPIN, 1967;

BROTHERS and RODGERS, 1969; DEN TEX, 1969). COLLÉE (1962) studied lherzolite nodules from Dreiser Weiher, Germany and from the Chaîne des Puys in Auvergne, France. He concluded that the lherzolite nodule from Auvergne is a secondary tectonite, the fabric of which can be explained as a result of rotation of pre-deformational fabric of the type observed in the sample from Dreiser Weiher. Judging from the total fabric, the peridotite nodule from Ichinomegata seems to differ from the lherzolite nodules studied by COLLÉE. BROTHERS and RODGERS (1969) noted that five orientation rules can be recognized for olivine in the ultramafic nodules from Auckland and that the enstatite fabric in the nodules shows no consistent relationship to the olivine fabric. AVE'LALLEMANT (1967) carried out the fabric analysis of lherzolites from the lherzolite-containing zone near Vicdessos, Ariège, France. According to him, the lherzolites of the zone have been folded isoclinally, and the axial-plane cleavage is almost always parallel to the compositional layering. He concluded that the orientation of olivine is directly dependent on the pre-Alpine axial-plane cleavage and only indirectly related to the layering and that the orientation patterns for X, Y, and Z of enstatite are in complete accordance respectively with the orientation of X, Y, and Z of olivine. Furthermore, he noticed that X, Y, and Z of diopside tend to be oriented respectively parallel to X, Y, and Z of olivine. The olivine fabrics of the lherzolites of that zone were divided by him into two types with a series of transition. Although the orientation patterns for X, Y, and Z of olivine of the lherzolitic peridotite nodule from Ichinomegata have a resemblance to those of olivine of the sample L-88 of harzburgitic lherzolite (AVE'LALLEMANT) from the Etang de Lers, the peridotite nodule from Ichinomegata, in respect to the total fabric, does not correspond to any one of many lherzolite samples described by AVE'LALLEMANT. The fabric of the ultramafic mass in the Higashiakaishiyama district, Japan, has been analyzed by YOSHINO (1961, 1964). Fresh specimens of massive dunite from the district consist almost entirely of equant grains of olivine, usually containing subordinate amounts of chromite and blade-shaped serpentine mineral. The olivine of the massive peridotite of Higashiakaishiyama shows the tendencies for the (010) plane to lie on a certain surface coinciding roughly with the compositional layering and for the [001] to be oriented parallel to a definite direction. Lattice orientation patterns of clinopyroxene in the clinopyroxene-bearing rocks occurring within the Higashiakaishiyama ultramafic mass bring out the tendencies for the (010) plane of clinopyroxene to lie on the surface coinciding roughly with the compositional layering and for the crystallographic c-axis of clinopyroxene to be oriented parallel to the definite direction coinciding with the [001] concentration in the olivine fabric patterns. In the Higashiakaishiyama ultramafic mass, the clinopyroxene fabric seems to be consistent with the olivine fabric. YOSHINO (1961, 1964) concluded that recrystallization or neocrystallization proceeding in a hydrous body under a tectonic condition must have been responsible for the development of the observed state of olivine fabric in the Higashiakaishiyama ultramafic mass. The fabric of olivine of the Ichinomegata peridotite nodule is

different from that of the Higashiakaishiyama massive peridotite. It appears that the orienting process related to the observed olivine fabric in the Ichinomegata peridotite nodule differs from the orienting process related to the olivine fabric in the Higashiakaishiyama peridotite. The difference may be attributed to the difference in physicochemical conditions as well as in the rate of deformation. Judging from the fact that the lattice orientation of olivine in the peridotite nodule is not always consistent with the grain boundary fabric, the development of the olivine fabric seems to have been accompanied by grain deformation. It is to be noted that serpentine mineral can hardly be found in the peridotite nodule. The observed fabric of olivine in the Ichinomegata peridotite nodule may have evolved under dry condition.

Recently, deformation experiments have been carried out on the peridotite minerals, and slip systems and deformation structures in the crystals of olivine, enstatite, and diopside have been discussed in detail (GRIGGS, TURNER, and HEARD, 1960; TURNER, HEARD, and GRIGGS, 1960; BORG and HANDIN, 1966; RALEIGH and TALBOT, 1967; RALEIGH, 1967, 1968; YOUNG, 1969; CARTER and AVE'LALLEMANT, 1970). KAMB (1956) discussed on the preferred orientation developed through crystallization under nonhydrostatic stress from the thermodynamic point of view. AVE'LALLEMANT and CARTER (1970) discussed textures and fabrics produced by syntectonic recrystallization of olivine in dunite and in olivine powder. It is difficult, however, to infer the state of stress influenced the structural evolution of the Ichinomegata peridotite nodule. The set of S_1, S_2, and S_3 has three mutually perpendicular symmetry planes, *ab*, *bc*, and *ac*. Therefore, the symmetry of stress system related to the development of the set of S_1, S_2, and S_3 is orthorhombic. The greatest stress axis and the least stress axis would be parallel to *c* and *b* respectively. The statistical *s*-surfaces, S_1', S_2', and S_3', however, must have deviated, respectively, from S_1, S_2, and S_3 through rotation, and, consequently, the symmetry of the set of S_1', S_2', and S_3' must have become monoclinic. Formations of the orthorhombic fabric (S_1, S_2, and S_3) and the monoclinic fabric (S_1', S_2', and S_3') have been followed by the development of the strain-slip structure, S_4, intersecting *a*, *b*, and *c* obliquely.

The following history of deformation can be drawn for the Ichinomegata lherzolitic peridotite nodule from the results of petrofabric studies.

1. *The earlier phase*

Aggregates of orthopyroxene, clinopyroxene, and spinel would have occurred as parallel layers (S_L) in the matrix of olivine aggregate. Both pyroxenes show common tendencies for the (010) plane to lie parallel to the surface of compositional layering and for the crystallographic c-axis to be oriented parallel to a definite direction which defines a statistical linear structure on the surface of layers. The crystallographic a-axis of olivine shows the tendency to be oriented parallel to the

linear structure. These fabrics would have been developed as the result of flow through the earlier phase.

2. *The later deformation*

In the later phase, the rock has been influenced by the stress system with the greatest stress axis oriented roughly parallel to the earlier layers and normal to the earlier linear structure. Defining *ab*, the foliation (S_1) parallel to the earlier lineation has been developed approximately normal to the greatest stress axis. Simultaneously with the development of S_1, conjugate *s*-surfaces, S_2 and S_3, have been formed, symmetrically intersecting S_1 in a common axis defining *b*. Such deformation, accompanied by grain deformation and recrystallization, has been imposed on the fabric of the earlier phase, represented by the preferred location of different direction groups of olivine and by the grain boundary fabric of the mineral. Closely related to the development of S_1, S_2, and S_3, the preferred lattice orientation of olivine has evolved. The statistical *s*-surfaces, S_1', S_2', and S_3', related respectively to S_1, S_2, and S_3, have been defined by the preferred orientation of the (001) plane of olivine belonging to the different individual direction groups. S_1', S_2', and S_3' have deviated respectively from S_1, S_2, and S_3 through rotation, and the symmetry of the set of S_1', S_2', and S_3' has become monoclinic. Formations of the orthorhombic fabric (S_1, S_2, and S_3) and the monoclinic fabric (S_1', S_2', and S_3') have been followed by the development of the strain-slip structure S_4 intersecting *a*, *b*, and *c* obliquely. Grains of both pyroxenes have been partly distorted, and their lattice orientation has hardly been influenced in response to the condition of the later deformatiton. The preferred lattice orientation of both pyroxenes survives as inherited structure. The deformation of this phase has proceeded under dry condition.

The history of deformation as outlined above implies that the peridotite nodule has been translated and rotated under the stress condition, that giving support to Kuno's opinion (KUNO, 1967). This peridotite nodule can be regarded as a fragment of the upper mantle material, and the fabric of the rock would have evolved through the flow within the upper mantle.

SUGIMURA and UYEDA (1967) discussed the anisotropy in the upper mantle under the island arcs. If the information on the attitude of olivine fabrics in the upper mantle under the Ichinomegata area is obtained, the pattern of movement and the state of stress of this part will be clarified. VERMA (1960) measured elastic wave velocities in the crystallographic directions of olivine, and the compressional wave velocities were reported to be 9.87, 7.73, and 8.65 km/sec in the [100], [010], and [001] directions respectively. KAWAHARA, SUZUKI, KUMAZAWA, KOBAYASHI, and IIDA (1968) showed that the anisotropism for the P-wave in the Horoman dunite from Hidaka-zone, Hokkaido, is closely related to the preferred orientation of olivine in the dunite. The anisotropic fabric defined by the lattice orientation of olivine in the Ichinomegata peridotite nodule should be reflected on the anisotropy with

respect to the compressional wave velocity in the peridotite. Therefore, factual data on the anisotropy for seismic wave velocities in the upper mantle under the Japanese island arc are required for the discussion on this problem.

LITERATURES

AVE'LALLEMANT, H. G. (1967): Structural and petrofabric analysis of an "Alpine-type" peridotite: The lherzolite of the French Pyrenees. *Leidse Geol. Mededel.*, **42**, 1-57.

——— and CARTER, N. L. (1970): Syntectonic recrystallization of olivine and modes of flow in the upper mantle. *Geol. Soc. America Bull.*, **81**, 2203-2220.

BATTEY, M. H. (1960): The relationship between preferred orientation of olivine in dunite and the tectonic environment. *Amer. Jour. Sci.*, **258**, 716-727.

BORG, I., and HANDIN, J. (1966): Experimental deformation of crystalline rocks. *Tectonophysics*, **3**, 249-368.

BROTHERS, R. N. (1959): Flow orientation of olivine. *Amer. Jour. Sci.*, **257**, 574-584.

——— (1964): Petrofabric analyses of Rhum and Skaergaard layered rocks. *Jour. Petrology*, **5**, 255-274.

——— and RODGERS, K. A. (1969): Petrofabric studies of ultramafic nodules from Auckland, New Zealand. *Jour. Geology*, **77**, 452-465.

CARTER, N. L., and AVE'LALLEMANT, H. G. (1970): High temperature flow of dunite and peridotite. *Geol. Soc. America Bull.*, **81**, 2181-2202.

COLLÉE, A. L. G. (1962): A fabric study of lherzolites, with special reference to ultrabasic nodular inclusions in the lavas of Auvergne (France). *Leidse Geol. Mededel.*, **28**, 1-102.

DEER, W. A., HOWIE, R. A., and ZUSSMAN, J. (1963): *Rock-forming minerals. II. Chain silicates.* London, Longmans, Green and Co., 8-9.

DEN TEX, E. (1969): Origin of ultramafic rocks, their tectonic setting and history: A contribution to the discussion of the paper "The origin of ultramafic and ultrabasic rocks" by P. J. Wyllie. *Tectonophysics*, **7**, 457-488.

ERNST, T. (1935): Olivinknollen der Basalte als Bruchstücke alter Olivinfelse. *Nachr. Ges. Wiss. Göttingen, Math. Physik. Kl. IV, Geol. Mineral.*, **1**, 147-154 (Cited in ERNST, T., 1967).

——— (1967): Olivine nodules and the composition of the Earth's mantle, in RUNCORN, S. K., ed., *Mantles of the Earth and Terrestrial Planets.* New York, John Wiley and Sons, 321-328.

FAIRBAIRN, H. W. (1949): *Structural Petrology of Deformed Rocks.* Cambridge, Mass., Addison and Wesley Publishing Co.

GRIGGS, D. T., TURNER, F. J., and HEARD, H. C. (1960): Deformation of rocks at 500° to 800°C. *Geol. Soc. America Mem. 79*, 39-104.

HAYASHI, H. (1955): Ejecta around Itinome-gata in Oga Peninsula, Akita Prefecture (in Japanese). *Jour. Geol. Soc. Japan*, **61**, 240-248.

KAMB, W. B. (1959): Theory of preferred crystal orientation developed by crystallization under stress. *Jour. Geology*, **67**, 153-171.

KASAHARA, J., SUZUKI, I., KUMAZAWA, M., KOBAYASHI, Y., and IIDA, K. (1968): Anisotropism of P-wave in dunite (in Japanese). *Jour. Seism. Soc. Japan.* Ser. 2., **21**, 222-228.

KOJIMA, G., and HIDE, K. (1957): On new occurrence of aegirine augite-amphibole-quartz-schists in the Sambagawa crystalline schists of the Besshi-Shirataki district, with special reference to the preferred orientation of aegirine augite and amphibole. *Jour. Sci. Hiroshima Univ.*, Ser. C, **2**, 1-20.

——— ——— (1958): Kinematic interpretation of the quartz fabric of triclinic tectonites from Besshi, Central Shikoku, Japan. *Jour. Sci. Hiroshima Univ.*,. Ser. C, **2**, 195-226.

KUNO, H. (1967): Mafic and ultramafic nodules from Itinome-gata, Japan, in WYLLIE, P. J., ed., *Ultramafic and Related Rocks.* New York, John Wiley and Sons, 337-342.

LADURNER, J. (1954): Das Verhalten des Olivines als Gefügekorn in einigen olivingesteinen. *Tschermaks Miner. Petr. Mitt.* (3d. Ser.), **5**, 21-36.

LAPPIN, M.A. (1967): Structural and petrofabric studies of the dunites of Almklovdalen, Nordfjord, Norway, in WYLLIE, P.J., ed., *Ultramafic and Related Rocks.* New York, John Wiley and Sons, 183-190.

PAULITSCH, P. (1953): Olivinkornregelung und Genese des Chromitführenden Dunits von Anghida auf der Chalkidike. *Tschermaks Miner. Petr. Mitt.* (3d. Ser.), **3**, 158-166.

RALEIGH, C.B. (1967): Experimental deformation of ultramafic rocks and minerals, in WYLLIE, P.J., ed., *Ultramafic and Related Rocks.* New York, John Wiley and Sons, 191-199.

——— (1968): Mechanisms of plastic deformation of olivine. *Jour. Geophys. Research*, **73**, 5391-5406.

——— and TALBOT, J.L. (1967): Mechanical twinning in naturally and experimentally deformed diopside. *Amer. Jour. Sci.*, **265**, 151-165.

SUGIMURA, A., and UYEDA, S. (1967): A possible anisotropy of the upper mantle accounting for deep earthquake faulting. *Tectonophysics*, **5**, 25-33.

TURNER, F.J. (1942): Preferred orientation of olivine crystals in peridotites, with special reference to New Zealand examples. *Royal Soc. New Zealand Trans.*, **72**, 280-300.

——— HEARD, H., and GRIGGS, D.T. (1960): Experimental deformation of enstatite and accompanying inversion to clinoenstatite. *Internat. Geol. Congress, 21st, Norden*, Part 18, 399-408.

——— and WEISS, L.E. (1963): *Structural analysis of metamorphic Tectonites.* New York, McGraw-Hill Book Co.

VERMA, R.K. (1960): Elasticity of some high-density crystals. *Jour. Geophys. Research*, **65**, 757-766.

YOSHINO, G. (1961): Structural-petrological studies of peridotite and associated rocks of the Higashiakaishi-yama district, Shikoku, Japan. *Jour. Sci. Hiroshima Univ.*, Ser. C, **3**, 343-402.

——— (1964): Ultrabasic mass in the Higashiakaishiyama district, Shikoku, Southwest Japan. *Jour. Sci. Hiroshima Univ.*, Ser. C, **4**, 333-364.

YOUNG, C. (1969): Dislocations in the deformation of olivine *Amer. Jour. Sci.*, **267**, 841-852.

DEPARTMENT OF GEOLOGY
SHINONOME BRANCH SCHOOL
HIROSHIMA UNIVERSITY

Explanation of Plate XVI

Fig. 1. Cut surfaces of the specimen of analysed peridotite nodule (HK 63111602).

Fig. 2. Photomicrograph of olivine. Thin section No. GYHK 63111602(5-1); nicols crossed.

Fig. 3. Photomicrograph of olivine and orthopyroxene. Thin section No. GYHK 63111602(1); lower nicol only. Ol: olivine; Opx: orthopyroxene.

Fig. 4. Photomicrograph of olivine, orthopyroxene, and clinopyroxene. Thin section No. GYHK 63111602(5-1); nicols crossed. Ol: olivine; Opx: orthopyroxene; Cpx: clinopyroxene.

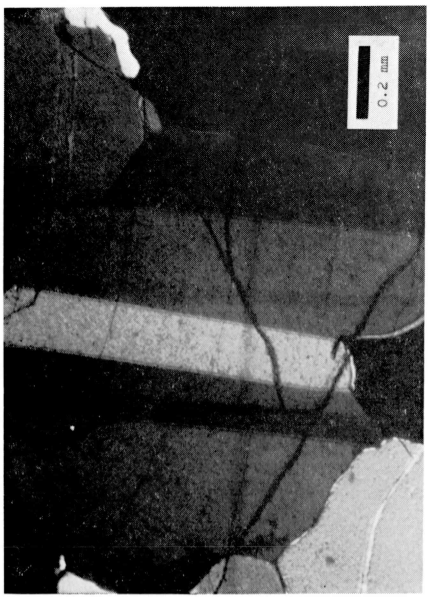

FIG. 2

FIG. 4

FIG. 1

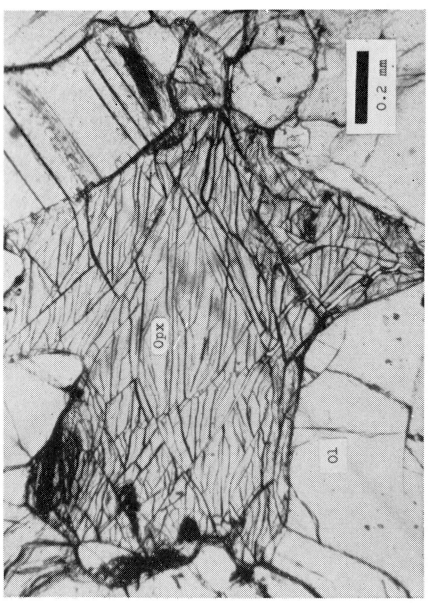

FIG. 3

Explanation of Plate XVII

Part of the specimen of analysed peridotite nodule.

A. Three cut surfaces.

B. Original surface.

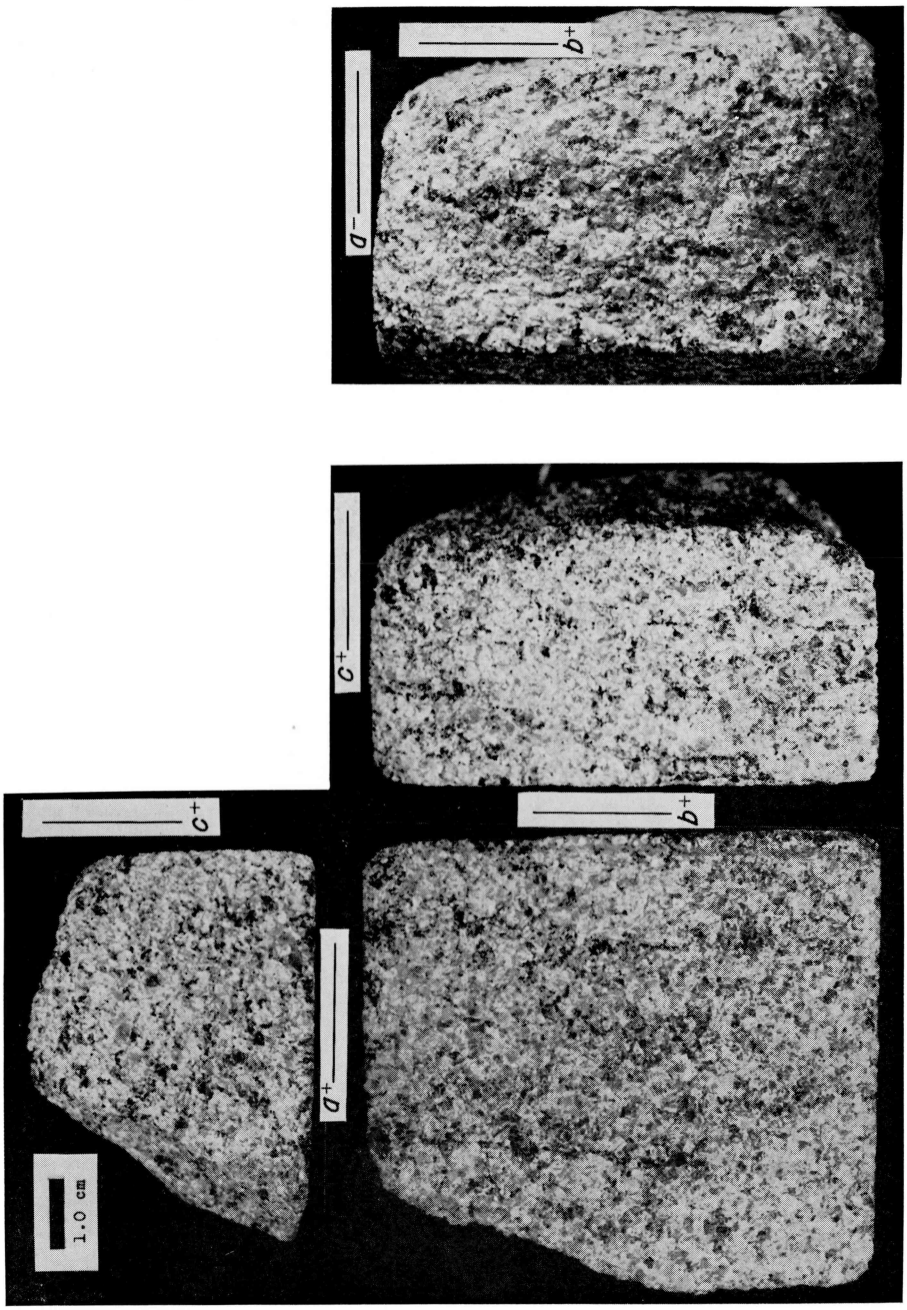
a−
b+
B
c+
b+
c+
a+
1.0 cm
A